Salt Tectonics of the Offshore Tarfaya Basin, Moroccan Atlantic margin

Rodolfo M. Uranga[1,]; Oriol Ferrer[1]; Gonzalo Zamora[2]; Josep A. Muñoz[1]; Mark G. Rowan[3]*

[1] Departament de Dinàmica de la Terra i de l'Oceà, Facultat de Ciències de la Terra, Universitat de Barcelona, Martí i Franquès s/n, 08028 Barcelona, Spain

[2] Repsol, Méndez Álvaro, 44, 28045 Madrid, Spain

[3] Rowan Consulting, Inc. 850 8th St., Boulder, CO 80302, USA

[*] Corresponding author: ruranga@ub.edu

Abstract

Salt tectonics play a critical role on passive margins evolution controlling aspects like structural style, subsidence patterns and thermal history, amongst others. The salt-bearing Atlantic passive margin of Morocco hosts one of the oldest stratigraphic records documenting the opening history of the Central Atlantic. However, the available seismic data is scarce and some offshore basins are still poorly studied, particularly in southern Morocco. Through the interpretation of an unpublished 2D/3D seismic dataset from the offshore Tarfaya Basin (SW Morocco), this study aims to highlight the key events that conditioned the evolution of this salt-bearing basin. From proximal to distal regions, the structural style of the basin is characterized by expulsion rollovers and salt-cored anticlines delimited by primary welded surfaces, evolving to buried salt sheets surrounded by thick minibasins and finally, diapirs actively deforming the modern seabed. From Late Triassic to Early Jurassic times, salt was deposited with a basinward thickening wedge-shaped geometry on a narrow trough developed over thinned continental crust. During the Jurassic, sedimentation and associated salt withdrawal triggered early salt deformation. Gravity gliding is a common process in salt-bearing passive margins that requires an originally continuous autochthonous salt layer with a minimum slope angle and longitude to thickness ratio of the overburden. However, in the Tarfaya Basin, the narrow geometry of the salt-bearing depocenter hampered this process. Early salt tectonics was probably triggered by slope progradation during the Early Jurassic. During the Early Cretaceous, the progradation of the Tan-Tan Delta promoted a continued basinward expulsion of salt, the development of a local salt-detached gravitational system and the proximal extrusion of salt sheets. Finally, from Late Cretaceous to the Present-day, shortening related to the convergence between Africa and Eurasia resulted in thick-skin inversion and the rejuvenation of precursor salt structures.

Key words: *Salt tectonics, Tarfaya Basin, Rifted passive margins, Central Atlantic, Morocco, Basin evolution*

1. Introduction

The Atlantic passive margin of Morocco extends for more than 1000 km and involves the largest salt basin in NW Africa containing one of the oldest stratigraphic records documenting the opening history of the Central Atlantic (Lancelot and Winterer, 1980; Seibold, 1982; Davison, 2005; Tari and Jabour, 2013; Tari et al., 2017). During Triassic times, extensional basins developed along the future continental margin and in the Atlas rift system (Dillon, 1974; Uchupi et al., 1976). The Tarfaya Basin (Ranke et al., 1982) extends over an area of approximately 50,000 km^2 (Fig. 1) between onshore and offshore southern Morocco and east of Fuerteventura and Lanzarote Islands (Spain). According to Tari et al. (2012a), the Tarfaya Basin conjugate margin corresponds to the southernmost region of the Nova Scotia Basin in Canada. Moreover, Tari et al. (2012a) and Louden et al. (2013) propose that the southern Nova Scotia and southern Morocco conjugate margins formed within the transition between a magma-rich segment to the south and a magma-poor segment to the north. Late Triassic (Rhaetian) to Early Jurassic (Hettangian) salt (Fig. 2) is interpreted to have been deposited during the late syn-rift stage prior to continental breakup (Hafid, 2000; Blackburn et al., 2013), i.e., during the crustal thinning stage (syn-thinning salt *sensu* Rowan, 2014). The lack of deep wells reaching the top of salt on a distal setting increases the uncertainty in establishing the age of salt.

Salt on rifted passive margins can be deposited during different stages during the rifting history (pre-rift, syn-rift and post-rift). This impacts on critical factors of salt tectonics evolution such as the prevalence of thick-skinned extension (typical of pre- and syn-rift salt) or thin-skinned gravity gliding (typical of post-rift salt) (Rowan, 2014). Moreover, the initial salt thickness and distribution patterns inherent to late syn-rift salt basins induce distinctive responses to well-known processes like basin tilting due to thermal subsidence or sediment progradation (Ge et al., 1997; Tari et al., 2003; Gaulier and Vendeville, 2005; Allen and Beaumont, 2016; Ferrer et al., 2017) and condition its subsequent evolution. In this context, the Tarfaya Basin constitutes an excellent research area for investigating the relationship between these processes from a salt tectonics perspective.

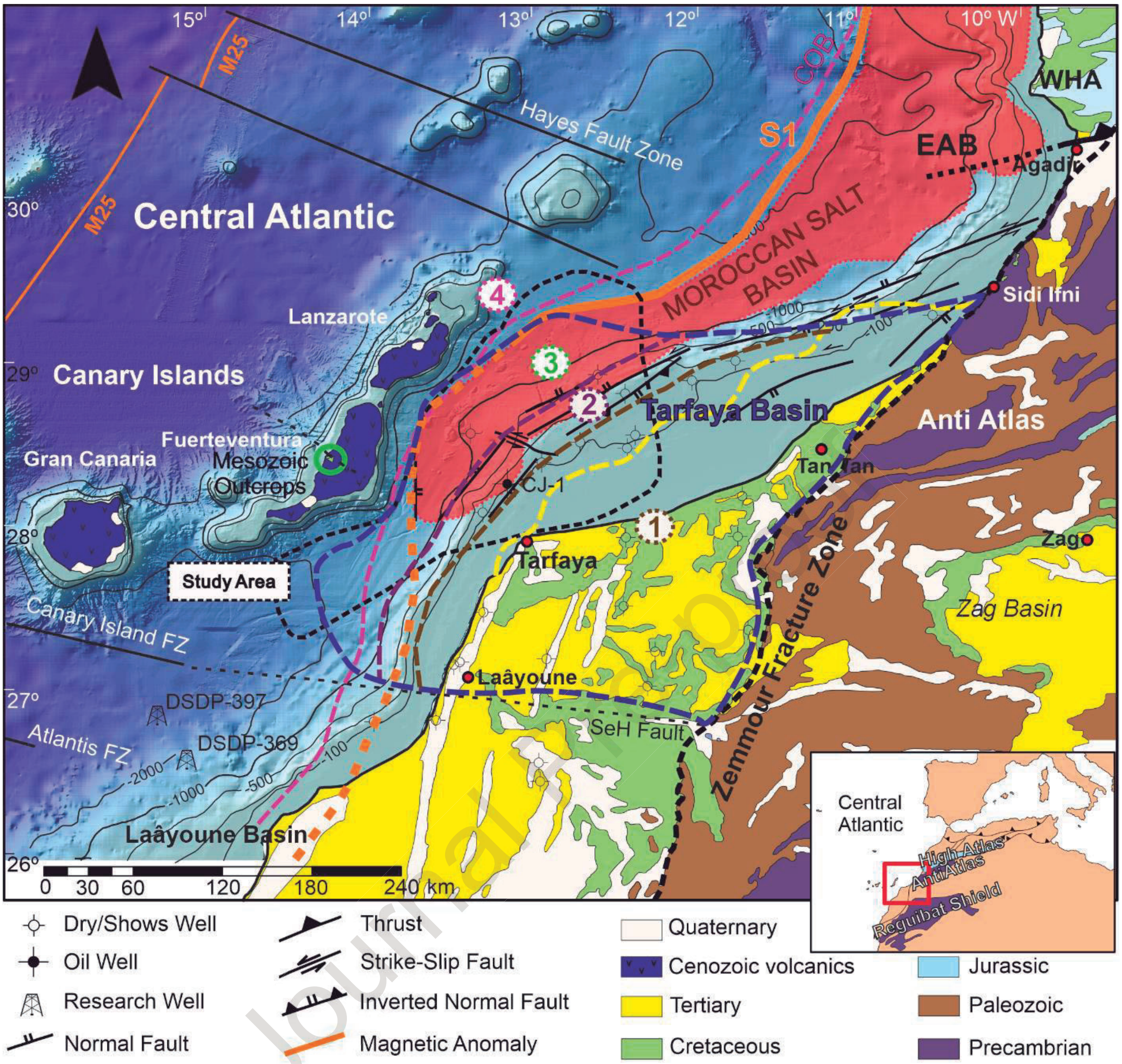

Figure 1. *Location map with main regional geological features modified from Wenke (2014). Numbers labeled 1 to 4 correspond to the "Unthinned crust", "Necking", "Thinned crust" and "Oceanic" domains (this study), respectively, modified from Le Roy & Piqué (2001). The dashed lines with the corresponding colors are the limits of each of these domains. COB: Continent-Ocean Boundary after Müller, et al. (2008); S1 magnetic anomaly after Roeser (1982); CJ-1: Cap Juby exploration well; Atlantic fault zones defined after Klitgord & Schouten (1986); WHA: Western High Atlas; EAB: Essaouira/Agadir Basin. The yellow dashed line corresponds to the shoreline position during Berriasian times (Tan-Tan Delta) following criteria proposed by Arantegui (2019).*

From a hydrocarbon potential perspective, southern offshore Morocco is underexplored. Only few exploration wells have been drilled, and most of them are located on the shelf. At least two working petroleum systems have been documented onshore (Broughton and Trepaniéré, 1993), in the Essaouira/Agadir Basin (EAB in future references) (Fig. 1). As for the Tarfaya Basin, the heavy oil discovery offshore Cap Juby in 1969 (CJ-1 in Fig. 1), although undeveloped, proved the presence of an active Jurassic-Jurassic and Jurassic-Cretaceous petroleum system (Sachse et al., 2016; Tari et al., 2012b; Tari and Jabour, 2013). The main reservoir facies tested were carbonate build-ups from the Lower and Middle Jurassic, but oil and gas shows were also described from Lower Cretaceous and Cenozoic sandstones (Morabet et al., 1998).

This study presents unpublished 2D and 3D seismic data calibrated with wells, together with structural and thickness maps to illustrate the main tectonostratigraphic features of the offshore Tarfaya Basin, focusing on the salt-bearing depocenter. Seismic interpretation and sequential structural restoration were carried out to understand the evolution of salt structures. Accordingly, this paper focuses on 1) the basement structure and its control on evaporite deposition; 2) the possible triggering mechanisms of salt tectonics; 3) the impact of deltaic progradation and shortening on precursor salt structures. The results offer a comprehensive guide that may lead to a better understanding of the kinematics and overall evolution of the offshore Tarfaya Basin, as well as serve as comparison with other neighboring salt-bearing basins such as the EAB.

2. Geological Setting

The pre-rift basement of the Tarfaya Basin consists of Paleozoic low-grade metasediments, deformed and metamorphosed during the Variscan (Fig. 2) orogeny (Lorenz, 1976; El Khatib and Ruellan, 1995; Piqué et al., 1998). The basin evolution started with the deposition of a Triassic - Lower Jurassic siliciclastic to evaporitic (mainly halite) syn-rift sequence (Hinz et al., 1982; Zühlke et al., 2004; Wenke et al., 2010). During this stage, sedimentation was controlled by grabens and half grabens striking in a general NE-SW direction (Le Roy and Piqué, 2001), inherited from the preexisting Paleozoic structural fabric. According to Le Roy et al. (1997), these structures are compatible with a WNW-ESE rifting axis. The Tarfaya Basin is segmented by fault accommodation zones striking in a general E-W direction (Heyman, 1989). One of these fault accommodation zones, the SeH fault (Fig. 1), marks the southern limit of the basin.

Le Roy and Piqué (2001) defined three main structural domains for the Tarfaya Basin: 1) An *external* (“*unthinned crust”* in this paper) domain in proximal areas (labeled 1 in Fig. 1) forming the substratum of the present coastal zone with an important basement control due to Variscan structural boundaries that were

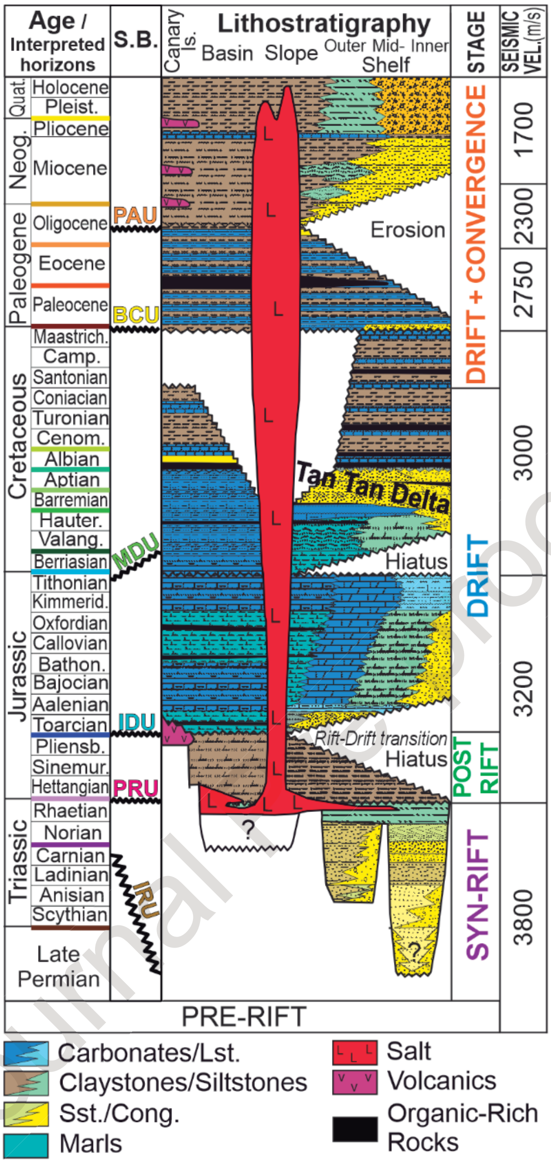

Figure 2. *Chronostratigraphic chart modified from Wenke (2014). Interpreted horizons are highlighted in 15 different colors (left). IRU: Initial Rift Unconf., PRU: Post-Rift Unconf., IDU: Initial Drift Unconf., MDU: Mature Drift Unconf., BCU: Base Cenozoic Unconf. (Neumaier et al., 2016), PAU: Peak Atlasian Unconformity.*

reactivated during the early rifting stage; 2) a *central* (referred as "*necking*" in this paper) domain (labeled 2 in Fig. 1) characterized by horsts and grabens that form the substratum of the present continental shelf break; and 3) an *inner* ("*thinned crust*" or also called *"Proto Atlantic Depocenter"* in this study, PAD in future references) domain in distal offshore areas (labeled 3 in Fig. 1), characterized by dominantly westward dipping faults. According to Le Roy and Piqué (2001), rifting began in the Early Triassic at the present-day Tarfaya Basin onshore region, where thick syn-rift strata is preserved in narrow half grabens bounded by E-dipping faults, and progressively migrated basinward. By the end of Carnian times, rifting was located at the necking domain and by Norian to Rhaetian times it affected the thinned crust domain in the distal offshore Tarfaya Basin. Rifting propagated not only westward but also northward through the EAB (Fig 1), resulting in extensional deformation acting on the entire margin during Rhaetian? – Hettangian times. Salt age determination in the Moroccan margin is based on studies in the onshore EAB where the uppermost evaporites are interfingered with dated basalts from the Late Triassic to Early Jurassic Central Atlantic Magmatic Province (Hafid, 2000; Tari et al., 2017), combined with data from four offshore wells (Hafid et al., 2008). However, great uncertainties arise when trying to date its basal section since no conclusive data is available (Fig. 6.4 in Hafid, et al., 2008). Moreover, onshore the EAB, salt deposition was controlled by N-S to NE-SW trending grabens with a patchy map-view character (Hafid et al., 2000; Hafid et al., 2006; Tari and Jabour, 2013; Tari et al., 2017; Pichel et al., 2019), adding great uncertainty to the correlation between distant salt basins.

During the Tarfaya Basin crustal thinning stage (Hettangian to Pliensbachian), thermal subsidence together with an eustatic sea level rise promoted the deposition of fine grained terrigenous clastics (Wenke, 2014). Although there is an ongoing debate on the timing of the onset of seafloor spreading and drifting (IDU in Fig. 2), most authors agree it took place between 190 and 170 Ma (i.e., between Pliensbachian and Bajocian times) (Klitgord and Schouten, 1986; Roeser et al., 2002; Sahabi et al., 2004; Davison, 2005; Labails et al., 2010; Sibuet et al., 2012). The S1 magnetic anomaly (Roeser, 1982; Roeser et al., 2002) coincides regionally with the transition between oceanic and continental crust (Fig. 1) and correlates suitably with the western border of the salt basin (Contrucci et al., 2004; Sahabi et al., 2004; Klingelhoefer et al., 2009; Lawrence, 2019). During Middle to Late Jurassic times, a passive margin sedimentary sequence was deposited consisting mainly of a prograding siliciclastic unit followed by proximal ramp and shelf carbonates (Fig. 2) grading distally to marls (Hinz et al., 1982; Ranke et al., 1982; Heyman, 1989; Le Roy and Piqué, 2001).

In Berriasian times, a basinwide regression exposed and eroded the Jurassic carbonate platform (MDU in Fig. 2) (Michard, 1976; Lancelot, 1977; Lancelot and Winterer, 1980; Wenke, 2014). The supplied sediments bypassed the shelf and formed the Tan-Tan Delta, active until Albian times (Martinis and Visintin, 1966; Ratschiller, 1970; El Khatib and Ruellan, 1995; Steiner et al., 1998; AbouAli et al., 2005; Arantegui, 2019). During the Late Cretaceous, the initial N-S oriented convergence between the Eurasian and African plates took place (Guiraud and Bosworth, 1997; Frizon de Lamotte et al., 2009; Neumaier et al., 2016). The low sedimentation rates combined with a eustatic sea level high stand (Haq et al., 1987) led to the deposition of a retrogradational to agradational sequence dominated by mudstones and calciturbidites (Wenke, 2014) with some influx of turbiditic sandstones in the offshore region (Steiner et al., 1998; García del Olmo et al., 2018; Martínez del Olmo, 2020).

Convergence between Africa and Iberia continued throughout the Cenozoic, promoting further uplift and erosion (Sehrt, 2014; Leprêtre et al. 2015; Gouiza et al., 2017). Evidence of this major tectonic event is the Base Cenozoic Unconformity (BCU in Fig. 2) which constitutes the most conspicuous erosional unconformity in the study area (Michard, 1976, Uchupi et al., 1976; Lancelot, 1977; Lancelot and Winterer, 1980; Stets and Wurster, 1982; El Khatib and Ruellan, 1995; Hafid et al., 2006; Hafid et al., 2008; Sehrt, 2014; Neumaier, 2016). Onlapping the BCU, the Paleogene deposits consist mainly of fine-grained clastic material (Wenke, 2014), with episodic inputs of turbiditic sandstones and calciturbidites in the deep offshore region (Martínez del Olmo, 2020). Well data collected from Sandia-1x (Fig. 3) show the presence of limestones with poor reservoir quality in the Paleocene-Eocene interval (García del Olmo et al., 2018), sand-rich turbidites with good reservoir characteristics in the Eocene-Miocene succession and mud-rich turbidites in the Pliocene-Recent interval (Hooghvorst et al., 2019).

Fuerteventura and Lanzarote islands represent the easternmost surface expressions of the Canary Islands volcanic province, which has been active since the Late Cretaceous (Anguita and Hernán, 2000, van den Bogaard, 2013). The islands and the associated crustal swell are caused by a sublithospheric thermal anomaly underlying oceanic crust regarded as the residue of an old mantle plume (Holik and Rabinowitz, 1991; Carracedo et al., 1998; Fullea et al., 2015). The Fuerteventura Jurassic to Cretaceous succession (Fig. 1) consist of vertical to overturned beds of Lower Jurassic normal mid-oceanic-ridge basalt (N-MORB) basalts and Jurassic to Cretaceous clastic and mixed deposits derived from the southwestern Moroccan continental margin (Robertson and Stillman, 1979; Steiner et al., 1998). The sedimentary succession overlies N-MORB flows and breccias representing the first stages of initial seafloor spreading in the Central Atlantic. According to Anguita and Hernán (2000) and Blanco-Montenegro et al. (2018), the exposure of this sedimentary succession is explained by the tectonic reactivation of a transfer zone (Fig. 1). This steeply dipping succession is unconformably overlain by Oligocene submarine volcanic rocks displaying a progressive unconformity. Finally, the climax of subaerial volcanic activity in Fuerteventura and Lanzarote islands took place between Miocene and Pleistocene times (e.g., Carracedo et al., 1998; Ancochea and Huertas, 2003).

Tectonic inversion and orogenesis of the Atlas system (i.e. High Atlas and Anti-Atlas, see Ruiz et al., 2011) took place during two distinct episodes: middle to late Eocene – Oligocene and late Miocene to Pliocene (Frizon de Lamotte et al., 2009). The earlier event was recorded in the Tarfaya Basin by the Peak Atlasian Unconformity (Fig. 2) (Wenke, 2014). Higher erosion rates related to the exhumation of the Atlas system (Wenke, 2014; Sehrt et al., 2018; Gouiza et al., 2017) and the Reguibat shield (Charton et al., 2021a) promoted an increase in sediment flux to the Tarfaya Basin. The transported sediments bypassed the shelf and were deposited at the slope and deep offshore regions as channelized turbiditic systems (García del Olmo et al., 2018; Martínez del Olmo, 2020).

3. Methodology

This study is based on the integration of zero-phase, time-migrated 2D and 3D reflection seismic data provided by REPSOL together with published well data compiled from 21 boreholes located mostly on the Moroccan shelf. The study area comprises 32,000 km^2 including the shelf, slope and deep offshore regions of the Tarfaya Basin. The 2D seismic dataset has a total length of 7,300 km, whereas the 3D seismic cube covers an area of 3,460 km^2 (Fig. 3).

The 2D seismic dataset is composed of different surveys with fair to good image quality, acquired between the 1970s and 2001 and reprocessed by Fugro-Geoteam. The 3D seismic volume was registered by PGS

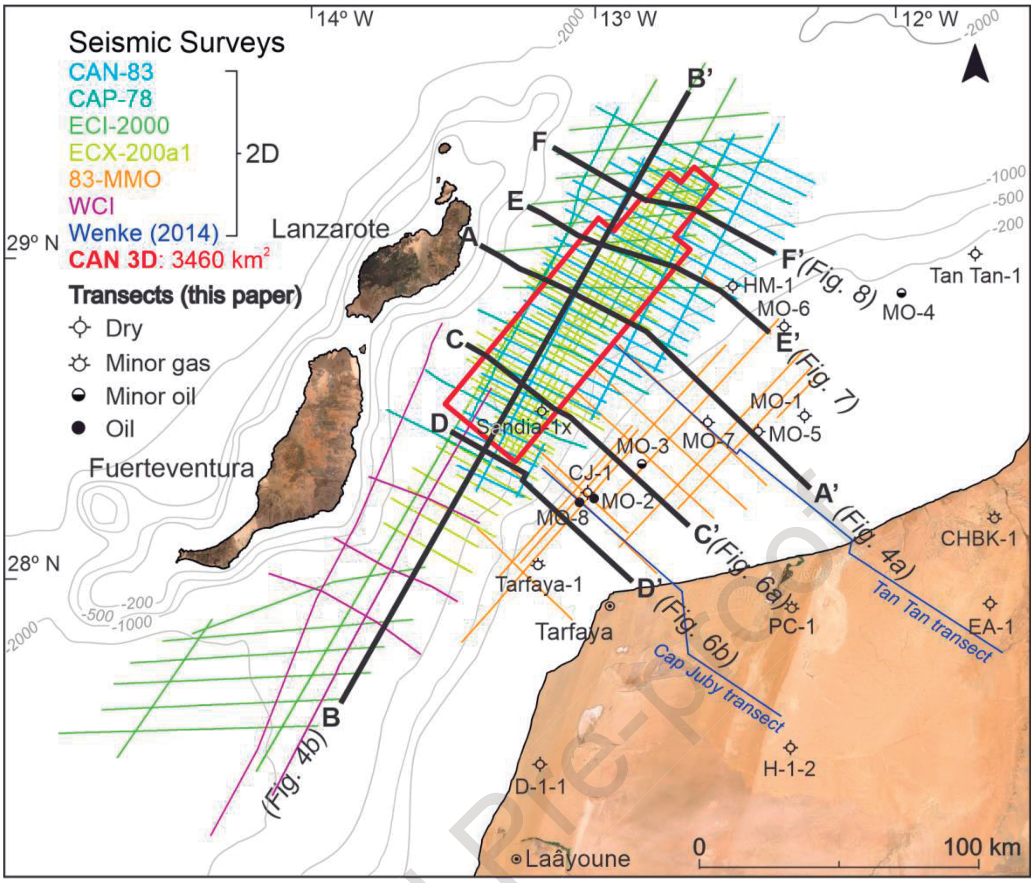

Figure 3. Well and seismic dataset. Highlighted in black are the seismic transects presented in this study.

exploration in 2003. During seismic processing, a Kirchoff pre-stack migration algorithm with a 4.5 km aperture was applied. The seismic data has a fold of 45 and was acquired with a recording time of 8.2 s. The volume has a very good image quality regarding the supra salt seismic reflections, whereas it deteriorates significantly in the pre-salt units (Fig. 4).

The seismic resolution is variable through the different surveys. On the 2D dataset, an average resolution of 15 m was calculated for the Cenozoic, considering an average seismic velocity of 2000 m/s, whereas for the Jurassic it is estimated to be 62 m considering an average seismic velocity of 3200 m/s. For the 3D data, an average resolution of 11 m was calculated for the Cenozoic and 35 m for the Jurassic. The velocity model was divided in six zones (Fig. 2) and was built combining well checkshot data from Wenke (2014) and VSP data from Sandia-1x well. Velocities were extrapolated following seismically continuous horizons interpreted in time domain. The seismic data is displayed following the SEG standard polarity convention, i.e., an increase in acoustic impedance with depth is represented by a positive reflection event (red color reflections on the seismic profiles). The 3D model velocities were obtained from checkshot data published by Wenke (2014) and integrated with well top information from El Khatib and Ruellan (1995). As a result, all the seismic transects presented through this study are depth converted.

A total amount of 15 horizons and 6 key unconformities (Fig. 2) were tied to wells using checkshot and VSP time/depth relationships and interpreted following criteria proposed by Wenke (2014) (Tan-Tan and Cap Juby transects in Fig. 3). Unconformities defined in the onshore and near offshore regions were extrapolated to the study area where most of them are represented by their corresponding correlative conformities. Volume attributes like structural smoothing, variance, spectral decomposition and TecVa (Bulhões and de Amorin, 2005) were calculated to aid in the seismic interpretation process, highlighting faults and salt bodies or improving the continuity of sub-salt reflectors where necessary. For structural restoration, the methodology of Rowan (1993) was followed, which incorporates isostatic compensation, decompaction, change in water depth and thermal subsidence. This workflow was implemented in 3D Move software (© Petroleum Experts).

4. Observations

In the following sections, a series of seismic transects and maps will be presented. Figure 4a illustrate the tectonic setting of the offshore Tarfaya Basin that will be described in this study: the distal PAD (= thinned domain), Cap Juby High region (CJH in Fig. 4a) (= necking domain) and the more proximal depocenters region (Tarfaya and Tan-Tan depocenters in Fig. 5, equivalent to the unthinned crustal domain).

4.1 Seismic Facies

The Paleozoic acoustic basement is characterized by reflectors with inhomogeneous and discontinuous seismic facies. However, some continuous sub-horizontal layering can be locally defined by high-amplitude reflections imaging metasedimentary units at the shelf region (Fig. 4a) with seismic velocities around 3800 m/s (Fig. 2). In contrast, on the northwestern deep offshore region of profile A-A' (Fig. 4a), basement reflections are characterized by transparent chaotic facies with no continuity. This subtle change in seismic facies coincides with the location of the S1 magnetic anomaly (Roesser et al., 2002).

The Triassic is seismically characterized by moderately continuous, heterogeneous, medium to high amplitude reflectors commonly displaying a wedge-shape geometry that either truncates or pinches-out against the acoustic basement. Two subunits can be differentiated (Fig. 2): a lower one (Carnian-Norian?) assigned to the initial phases of graben infill with a marked wedge-shaped geometry (syn-rift), and an upper one (Upper Triassic) that onlaps and covers basement highs (late syn-rift to post-rift) (Fig. 4). The Uppermost Triassic to Lower Jurassic evaporites are characterized by internally transparent, chaotic reflections with high reflectivity contrast with respect to the surrounding units. The presence of diapirs and salt sheets deteriorates the seismic quality of flanking and underlying units (Fig. 4).

The Jurassic units are characterized by medium amplitude, moderately continuous reflectors. Two subunits are interpreted: a Lower Jurassic succession (Hettangian – Pliensbachian), and a Middle to Upper Jurassic (Toarcian – Tithonian) interval (Fig. 4). From the analysis of the seismic sections, it can be noted an increase in the reflectors' continuity from the base to the top of the Jurassic. The Lower Jurassic unit shows significant thickness variations and onlap terminations, whereas the Middle to Upper Jurassic unit tends to truncate against diapirs' stems or secondary welded surfaces and displays a more isopachous character (Fig. 4).

The Cretaceous was subdivided into 6 units, separated by key tectono-stratigraphic surfaces (Fig. 2): Berriasian, Valanginian-Hauterivian, Barremian, Aptian, Albian and Upper Cretaceous. The basal contact is marked by an erosional unconformity, best imaged in the shelf region (MDU in Figs. 2 and 4a). The overall seismic character of the Cretaceous reflects fair to good continuity of the seismic events, with moderate amplitudes and major thickness variations in the pre-Aptian units. Moreover, reflector terminations of downlap, onlap and truncations related to a general progradational pattern are observed on the pre-Aptian succession in proximal settings (shelf and slope), whereas pseudo-clinoforms are identified basinward (Fig. 4a). In contrast, the post-Aptian units show a more isopachous character and reduced thickness. Reflectors

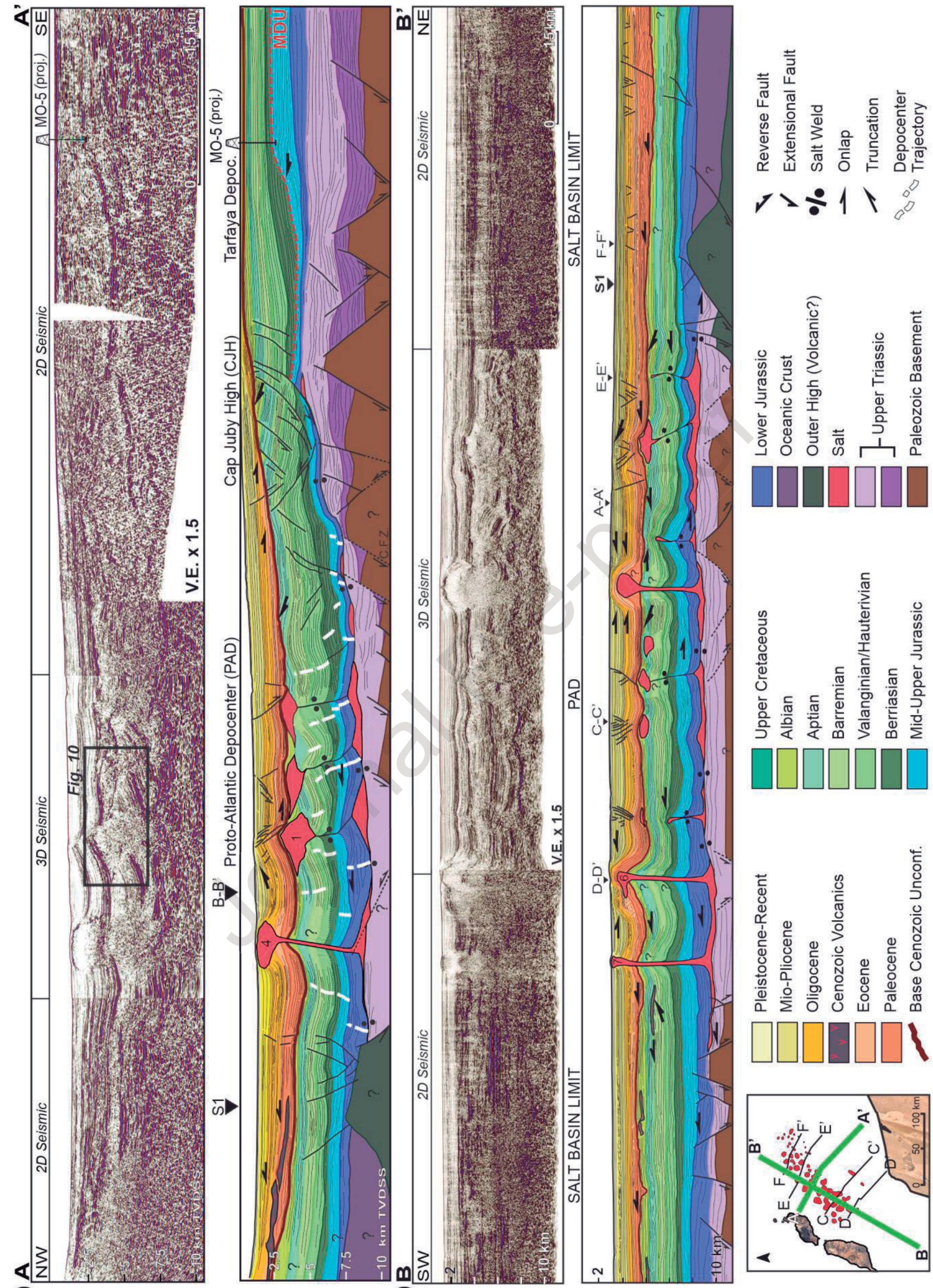

Figure 4. Depth converted uninterpreted and interpreted regional seismic transects. Vertical exaggeration (V.E.) x 1.5. Salt structures outlined in red on the location map. S1 refers to the location of the magnetic anomaly marking the COB (Continent-Ocean Boundary) (Roesser et al, 2002); C.F.Z.: Central Flexured Zone; **a)** Dip-oriented regional seismic transect A-A'. Outlined in black is the location of the salt structures illustrated on Figure 10; **b)** Strike-oriented profile B-B'. Diapirs labeled with numbers are described in section 4.3. For a high resolution version of this figure, please see the supplementary material.

246

terminations such as truncations against diapirs stems and onlaps against salt sheets are common. Truncations against the BCU are particularly frequent (Fig. 4). The Upper Cretaceous is preserved beneath the Base Cenozoic Unconformity in proximal areas.

Cenozoic seismic facies are characterized by low to moderate amplitude reflectors with good resolution and continuity. The unit is subdivided into five subunits (Figs. 2 and 4): Paleocene, Eocene, Oligocene, Mio-Pliocene, and Quaternary to Recent. A great variety of reflector terminations are noticeable, mainly onlaps and truncations related to the diapirs evolution. Moreover, stratigraphically constrained chaotic and discontinuous seismic facies are frequently observed in deep offshore region. Finally, it is important to note the presence of volcanic and intrusive bodies emplaced during the evolution and growth of the adjacent Lanzarote and Fuerteventura islands. These features, generally located in distal areas, show a high impedance contrast with the surrounding sediments, and are bounded by unconformities (Fig. 4a).

4.2 Regional Tectonic Features

The structural map of the top of acoustic basement (Fig. 5) shows a set of NE-SW trending horsts and half-grabens bounded by NW- and SE-dipping extensional faults (Figs. 4 and 5). These faults are mostly planar, with dipping angles ranging between 45 and 50º. Cap Juby High is the most prominent basement high in the basin, separating the salt bearing Proto Atlantic Depocenter (PAD in Fig. 5) to the west from the Tan-Tan and Tarfaya depocenters to the East where, presumably, no significant salt was deposited. Basinward of the Cap Juby High, the salt layer overlies a faulted basement covered by Triassic strata (Fig. 4). In general, basement faults do not offset the base of salt, except for major structures like the western faults bounding the Cap Juby High and faults marking the western limit of the PAD (Figs. 4, 6 and 7).

The top of the acoustic basement in the PAD lies more than 11 km below sea level. Although these depths are in agreement with published data (Heyman, 1989; Le Roy and Piqué, 2001; Gouiza, 2011), caution is required since no well has penetrated the complete sedimentary succession and the available seismic dataset do not

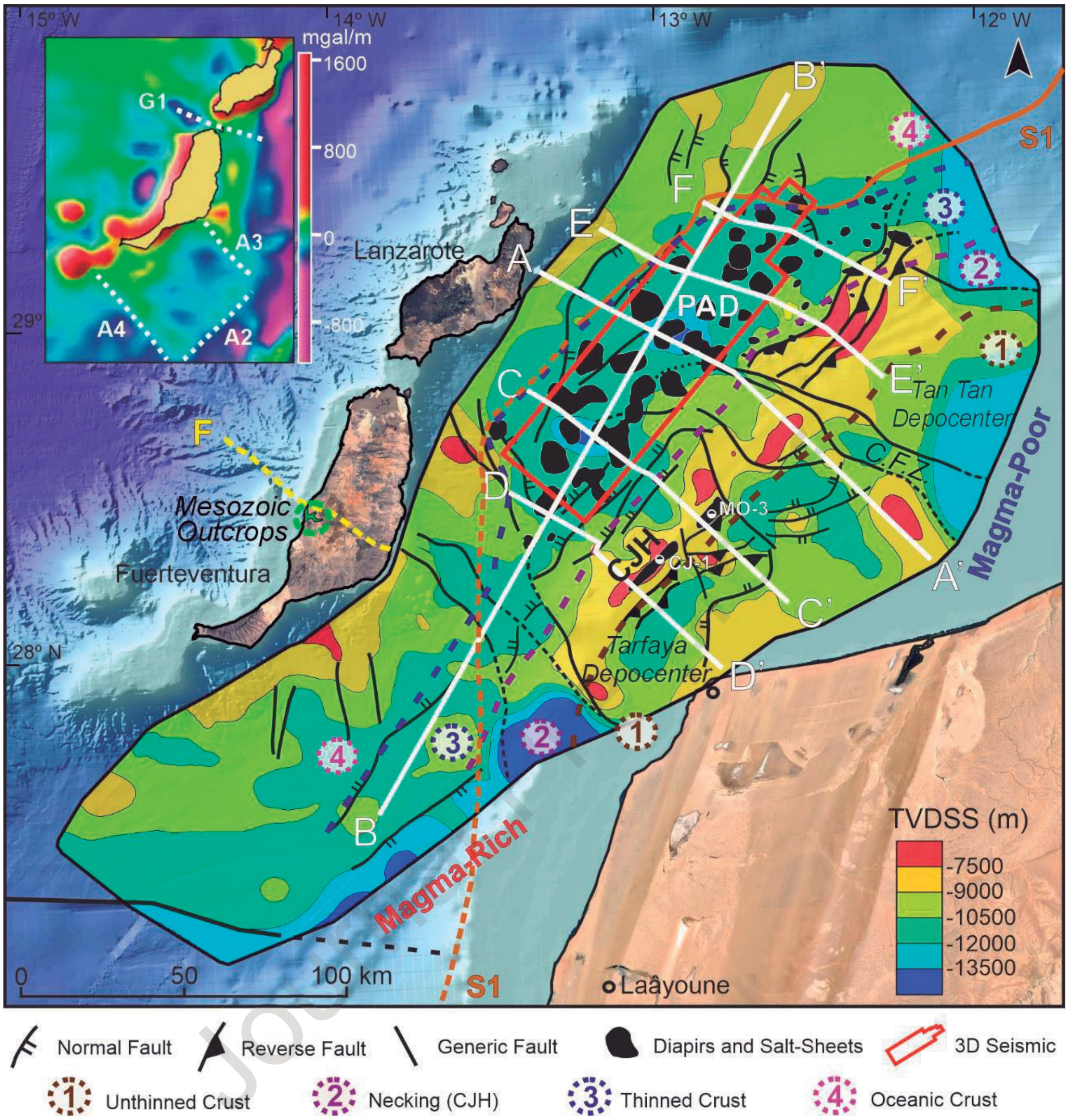

Figure 5. Depth structure map from the top of the acoustic basement. The lineament in Fuerteventura labeled "F" (Catalán et al, 2005) (yellow dashed line) is interpreted by the reference author as a possible deep-seated fault on magnetic data. C.F.Z.: Central Flexured Zone (Le Roy & Piqué, 2001); PAD: Proto Atlantic Depocenter. Wells CJ-1 and MO-3 reached the top of salt on the Cap Juby salt-cored anticline. Numbers labeled 1 to 4 and their correspondent thick dashed lines correspond to the tectonic domain boundaries of Le Roy and Piqué (2001). Inset shows a gravity anomaly map (modified from Carbó et al., 2003). The dashed white lines labeled A2 to A4 and G1 represent the edges of gravity highs matching possible fault bounded basement highs.

allow making confident velocity estimations. The distal limit of the PAD on profile A-A' (Fig. 4a) is marked by a set of chaotic reflectors and a step-up of the acoustic basement morphology from 11 to 8 km. This limit corresponds to a high-angle landward-dipping fault. Lower Jurassic (Sinemurian-Pliensbachian?) sediments onlap chaotic reflectors in the footwall of the fault interpreted as a volcanic? outer high.

The S1 magnetic anomaly (Figs. 1 and 5) coincides with the distal limit of the salt basin and is interpreted to represent the boundary between continental crust to the East and transitional/oceanic crust to the West (COB) (Hinz et al., 1982; Roesser et al., 2002; Contrucci et al., 2004). Following the criteria adopted by Louden et al. (2013), the Tarfaya Basin is located at the transition between a magma-poor rifted margin to the North and a magma-rich margin to the South. This classification is supported by the comparison of seismic refraction profiles on the North America and NW Africa conjugate margins (Klingelhoefer, et al., 2016; Biari et al., 2017) and by the presence of SDRs observed on deep seismic reflection profiles in the southernmost region of the conjugate Nova Scotia margin (Louden et al., 2013; Deptuck, 2020).

Basement highs bounded by NW-SE trending accommodation zones are interpreted on the southern limit of the salt basin and the PAD (Figs. 4b and 5). These structures have also been identified on gravimetric (upper left inset on Fig. 5) and magnetic surveys (Carbo et al., 2003; Catalán et al., 2003). The NW prolongation of these accommodation zones matches with the lineament bounding the steeply dipping and overturned Mesozoic sedimentary succession exposed on the western coast of Fuerteventura Island (Catalán et al., 2003; Steiner et al., 1998).

As shown in Figure 5, salt structures are mostly developed within the PAD, between the Cap Juby High to the East, which acted as a threshold controlling salt thickness during deposition, and the S1 anomaly to the West. However, some salt diapirs are also interpreted above the Cap Juby High (Figs. 5 and 6). These structures originated from the basinward expulsion of salt by the prograding wedge of Jurassic sediments (Fig. 6a). The reduced Upper Triassic thickness observed on profiles A-A’, C-C’ and D-D’ (Figs. 4a and 6) above the Cap Juby High indicates a lower accommodation space during this period and points to a high paleo-topography that controlled salt accumulation during the Late Triassic to Early Jurassic interval. Although no salt related seismic facies are observed in the Tarfaya depocenter, a primary weld and a related expulsion rollover is interpreted (Fig. 6a) pointing that, originally, a thin layer of salt was present in proximal settings (East from the MO-3 well in Fig 6a) and was expelled basinward during the Early Jurassic.

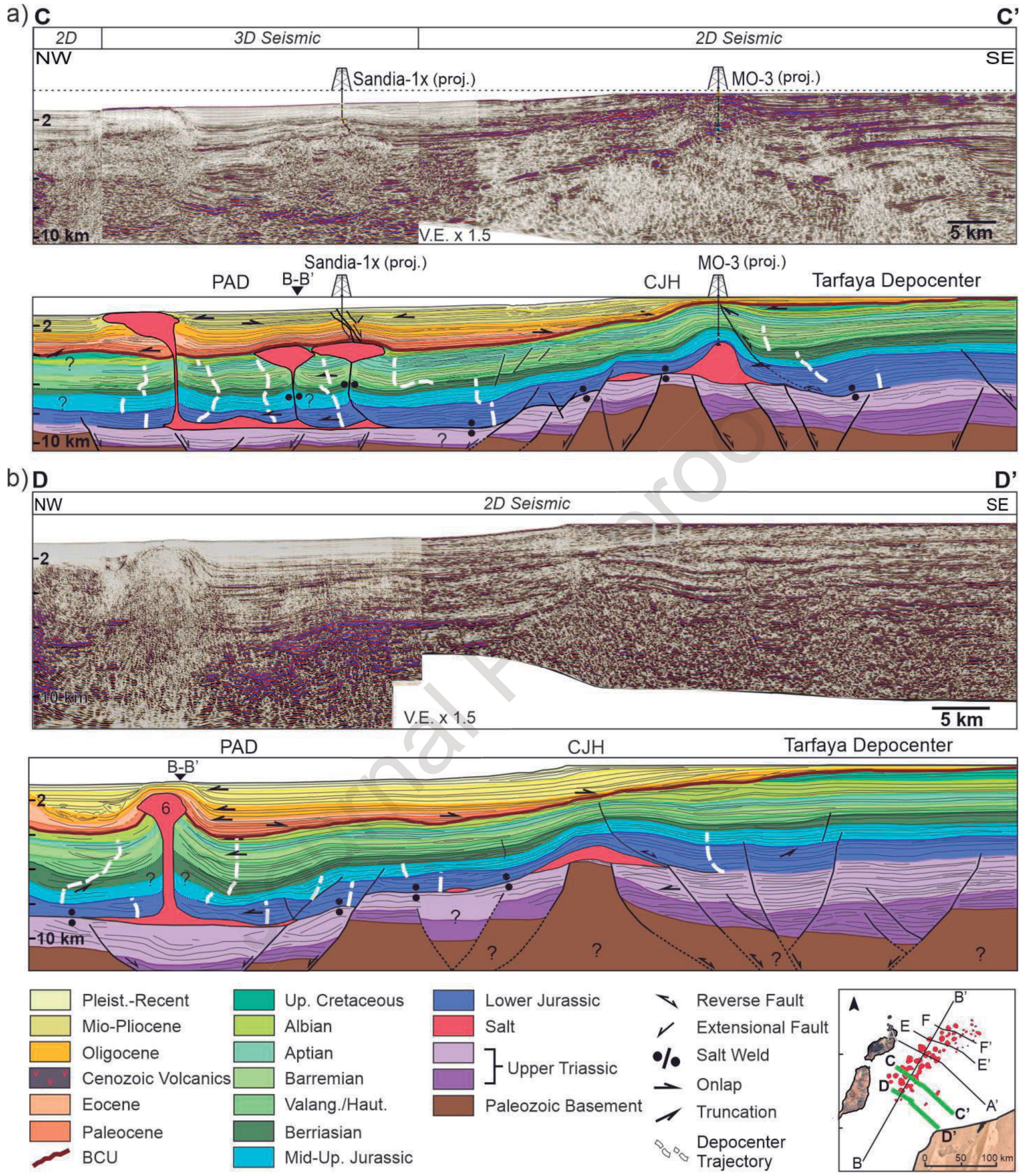

Figure 6. Uninterpreted and interpreted dip-oriented seismic transects. Vertical exaggeration (V.E.) x 1.5. CJH: Cap Juby High; PAD: Proto Atlantic Depocenter. a) profile C-C'; well MO-3 is projected 3.3 km and Sandia-1x is projected 3.9 km (see Fig. 3); at its actual location, drilling reached the top salt (Well TD represented by black dotted line). b) profile D-D'. Diapirs labeled with numbers are described in section 4.3. For a high resolution version of this figure, please see the supplementary material.

Figure 5 illustrates NE-SW trending basinward-vergent reverse faults bounding the CJH. To the southwest, these structures terminate against a fault accommodation zone that marks the limit of the PAD and the salt basin (Fig. 4b). Despite the low seismic resolution at basement levels, it is possible to interpret some of these deep-seated reverse faults, responsible for thick skinned inversion (for example, fault labeled “X” in fig. 7). Moreover, profile E-E’ (Fig. 7) shows a prominent slightly asymmetrical fault propagation fold involving Triassic strata related to this event. Also, on seismic transects C-C’, D-D’ (Fig. 6), E-E’ (Fig. 7) and F-F’ (Fig. 8), the Mesozoic succession on the eastern depocenter is structurally higher than in the PAD. Furthermore, it is possible to observe onlapping geometries of Paleocene to Lower Oligocene strata against the folded BCU.

4.3 Salt-Tectonic Features

One of the most important structures in the study area is the Cap Juby High, which is best illustrated on transects C-C’ and D-D’ (Fig. 6). On these profiles, the proximal region is characterized by a salt cored anticline located over CJH, called the Cap Juby anticline (Wenke, 2014), drilled by exploration wells MO-3 and CJ-1 (Figs. 3, 5 and 6a). These wells confirmed the top of salt and successfully tested hydrocarbons from Jurassic reservoirs (Morabet et al., 1998). Sigmoidal geometries of Lower Jurassic to Aptian growth strata bound this structure to the East with downlap terminations of Lower Jurassic reflectors against the Upper Triassic marking a primary weld (Fig. 6a). Moreover, a reverse fault cutting through this growth strata interval and detached on the primary weld is interpreted on the eastern flank of the anticline (Fig. 6). As modelling shows (Roma et al., 2018), this proximal primary welds can act as a decoupling layer between pre-salt and post-salt sediments as interpreted in Fig. 6. Basinward from the Cap Juby High, in the area corresponding to the present-day shelf break and slope, a prominent primary weld is oftenly overlain by salt pillows (Figs. 4a and 6). Further downdip, slightly asymmetrical salt pedestals which can reach up to 1.5 km of structural relief (Fig. 4) are separated by primary welds and overlain by onlapping thick Lower Jurassic successions (Figs. 4a and 9a).

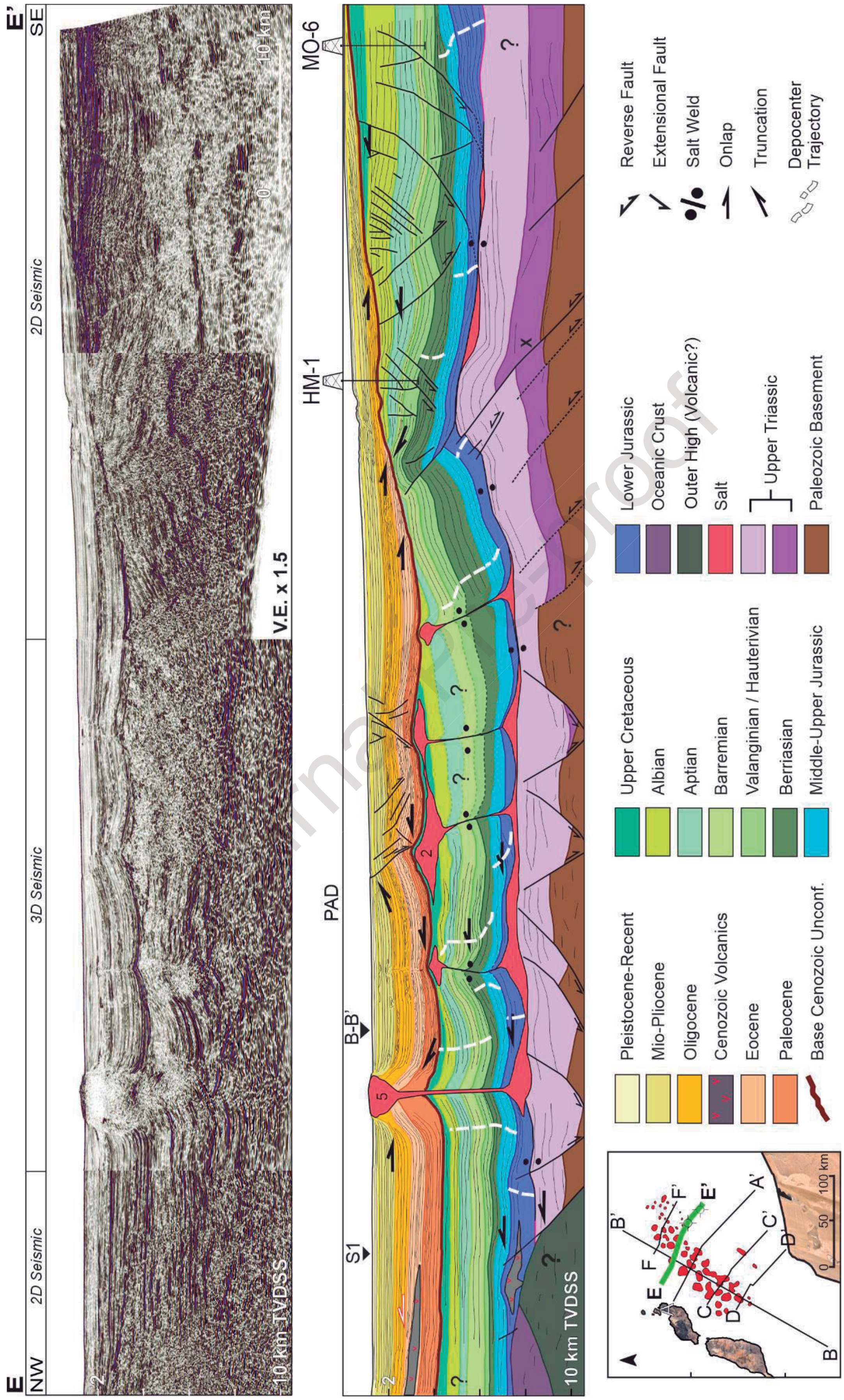

Figure 7. Uninterpreted and interpreted dip-oriented seismic transect E-E'. Vertical exaggeration (V.E.) x 1.5. Diapirs labeled with numbers are described in section 4.3. For a high resolution version of this figure, please see the supplementary material.

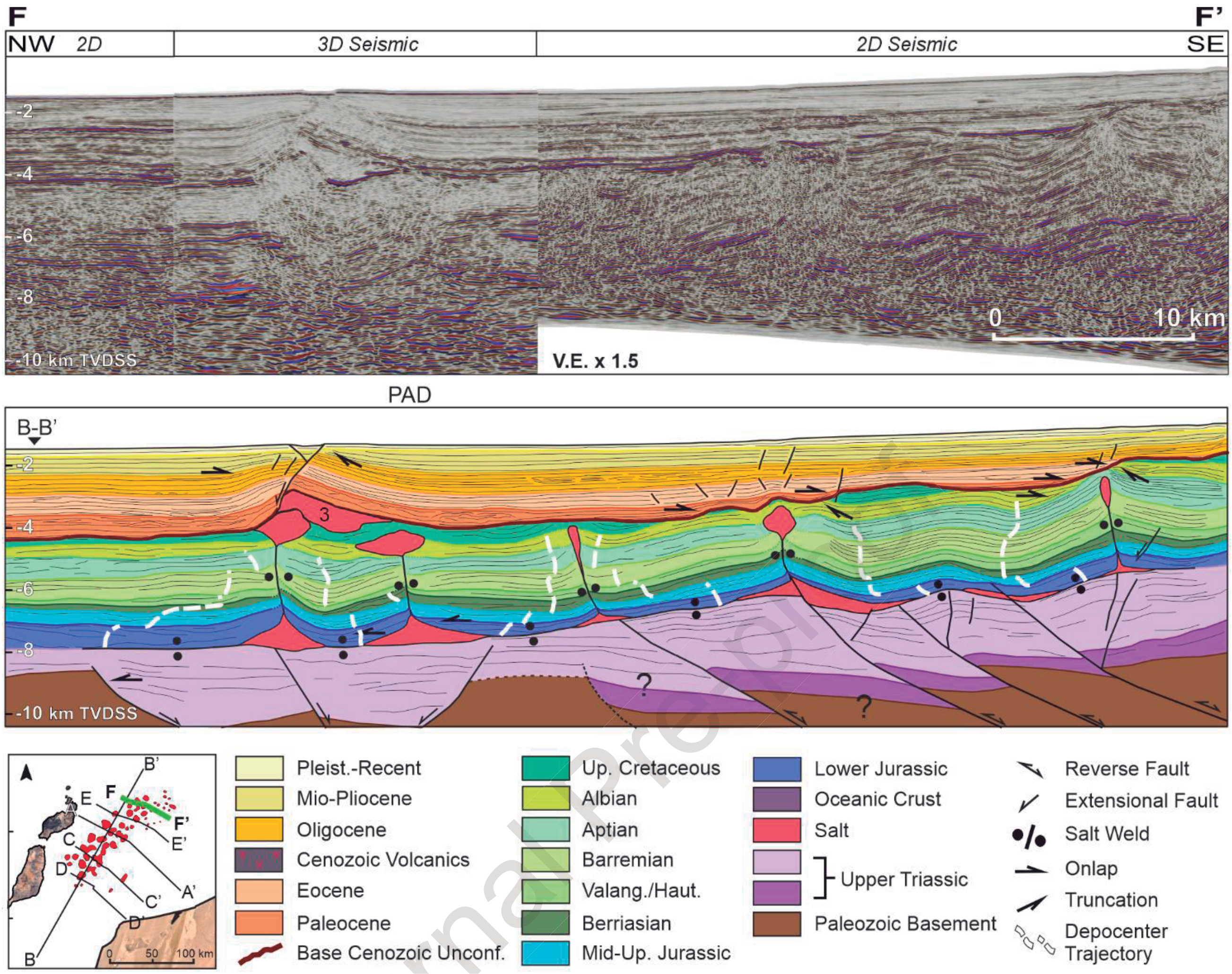

Figure 8. Uninterpreted and interpreted dip-oriented seismic transect F-F'. Vertical exaggeration (V.E.) x 1.5. Salt sheet labeled 3 is described in section 4.3. For a high resolution version of this figure, please see the supplementary material.

In the PAD, two main types of diapir stems can be described: near-vertical stems that are still open (mostly located distally) and counterregionally-dipping welded stems (mostly located proximally) (Fig. 9b). Both types are surrounded by long-lived (Jurassic to Present) minibasins, with maximum thicknesses of 8 km that have different geometries in the Mesozoic succession (Figs. 4a, 6a, 7 and 8). The vertical stems are flanked by depocenters whose axial-surface trajectories are stacked vertically or shift slightly landward up-section. In contrast, the counterregional welds separate minibasins with basinward shifting depocenters, forming pseudo clinoforms (Fig. 4a).

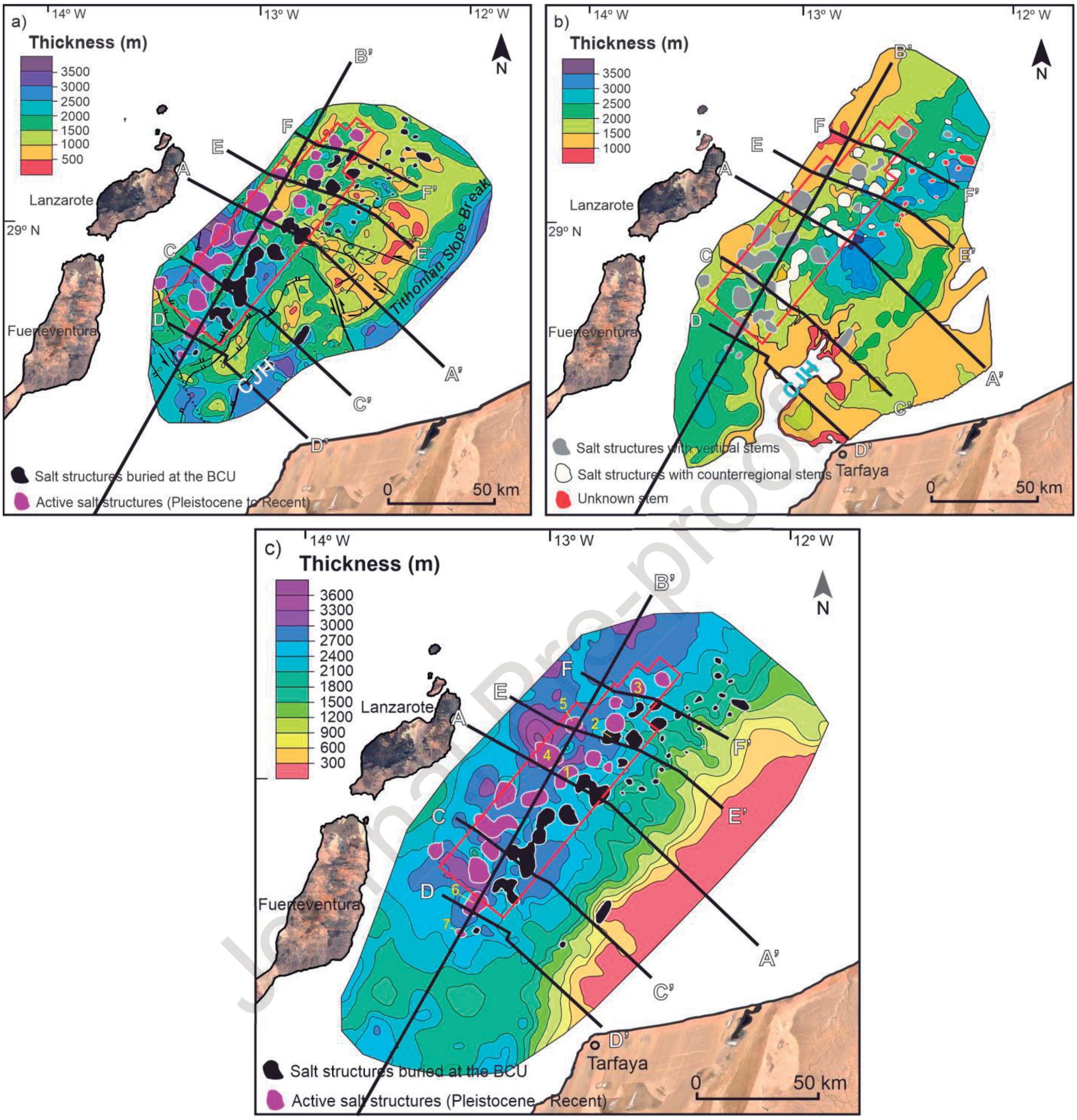

Figure 9. a) Jurassic vertical thickness map; CJH: Cap Juby High; **b)** Lower Cretaceous vertical thickness map (Tan-Tan Delta). CJH shows low sediment accumulation. Salt structures with counterregional stems tend to be in areas with thick accumulations related to the prograding Tan-Tan Delta; **c)** Cenozoic vertical thickness map. Cenozoic minibasins up to 3700 m thick are found in distal locations reflecting active salt related subsidence.

Lateral migration of depocenters is most prominent in the Lower Jurassic to Aptian interval. In both types of minibasins, the greatest thickness variations are observed in the Lower Jurassic interval (Figs. 4, 6 and 8). Regionally, Jurassic minibasins with a thicknesses ranging between 1500 m and 3600 m are located in the southern part of the PAD where vertical stems are predominant (Fig. 9a). In contrast, Lower Cretaceous minibasins with thicknesses between 1400 m and 3500 m characterize the proximal parts of central and northern areas of the PAD where counterregional welds and pseudo-clinoforms are common (Fig. 9b). The thickest Cenozoic minibasins are found distally (Fig. 9c), where open vertical stems are interpreted (Fig. 9b).

As observed in Fig. 9a (in black), a proximal fringe of salt sheets and diapirs underlies the BCU. Most of these structures are plug-fed salt sheets (Figures 4a, 7 and 8) that often coalesce to form canopies with landward dipping allosutures and counter-regionally dipping welded stems (Fig. 9b). These salt sheets are stratigraphically constrained in the Aptian - BCU interval. Figure 10 shows two of these salt sheets from

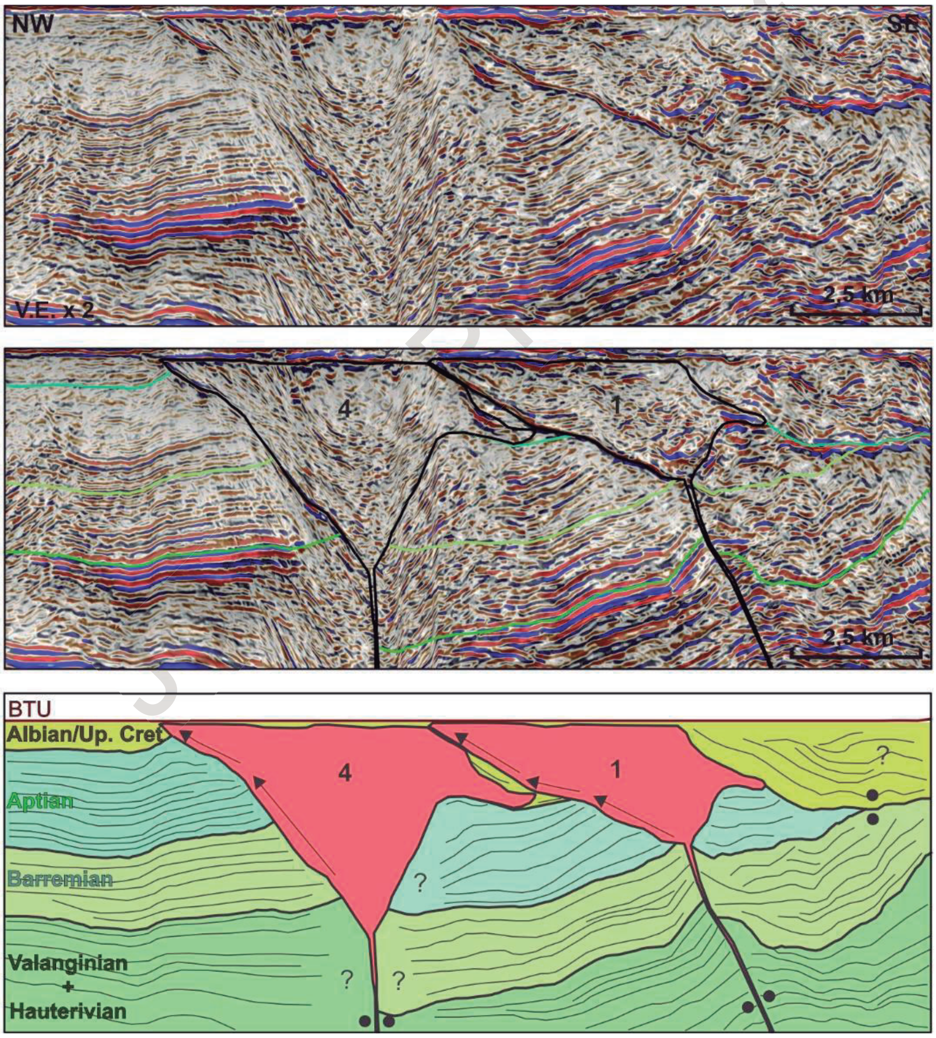

Figure 10. Seismic profile and detailed interpretation of the salt sheets from profile A-A' (Fig. 4a). The profile is flattened at the BCU. Arrows indicate basinward salt sheet advance. See section 4.3 for explanation.

profile A-A' (flattened to the BCU). The cutoffs at the base of the salt sheets show that lateral emplacement began during Barremian times for salt sheet 4 and during the Aptian for salt sheet 1. In general, these salt sheets and canopies exhibit thick Cenozoic roof strata folded above regional (e.g., see salt sheet 1 on Fig. 4a and salt sheet 2 on Fig. 7). Structures labeled 1, 2 and 3 (Figs. 4a, 7 and 8, respectively) share similar patterns of Cenozoic strata (for a map view of these structures see Fig. 9c): constant thickness for the Paleocene-Eocene interval, strata thinning onto the crests in the Oligocene and Mio-Pliocene intervals, and truncations against the base of the Pleistocene to Recent succession.

Further downdip, teardrop diapirs and minor salt sheets are observed. These structures, located at the most distal fringe of salt structures (in purple in Fig. 9c), have arched roofs, upturned collars and flaps and are actively deforming the seabed (relief > 400 m, see diapir 4 in Fig. 4a or diapir 5 on Fig. 7). Structures labeled 4 and 5 (Figs. 4a and 7 respectively) illustrate the Cenozoic stratal patterns of this distal fringe of structures: truncations against diapirs flanks for the Paleocene to lower Oligocene succession and onlapping geometries for the rest of the Cenozoic. Alternatively, in the southernmost sector of the study area, the Paleocene-Eocene succession onlaps and thins onto the salt (structures labeled 6 and 7 in Figs. 4b and 6b). Regionally, arched roofs from the more proximal salt sheets include almost the entire Cenozoic succession, whereas the distal fringe of diapirs have roofs with younger strata (Figs. 4, 7 ,8 and 6a). Moreover, the BCU is structurally above regional over the fringe of proximal buried salt sheets (e.g., salt sheet labeled 1 on Fig. 4a) and below regional in the Cenozoic minibasins flanking the most distal fringe of diapirs (e.g., minibasins flanking diapir 4 on Fig. 4a).

Even though an almost continuous layer of autochthonous salt is interpreted in the PAD and over Cap Juby High, there is only minor and local evidence for a salt-detached linked system of extension and contraction. Seismic transects A-A’ (Fig. 4a) and E-E´(Fig. 7) show a minor proximal peripheral graben, active during the Early Cretaceous, that marks the updip limit of the autochthonous salt. The small amount of extension (1,5 km for the peripheral graben of section A-A’) is only partially compensated basinward by subtle contraction (0,5 km). In section E-E’ (Fig. 7), shortening is evidenced by stratal thinning towards the anticline crest. Dating of the syn-shortening units is possible thanks to the stratigraphic information obtained from HM-1 well that documents a Valanginian/Hauterivian to up to, at least, Aptian age of the thinned succession (Fig. 7). However, a precise shortening interval cannot be reliably established due to the eroded stratigraphic record now represented by the BCU. Apart from these subtle features observed on profiles A-A' and E-E', no other evidence of a regional salt detached linked system is observed.

4.4 Regional Stratigraphic Trends

Wenke (2014) estimated sediment flux rates based on a reverse 2D flexural model following the methodology proposed by Bowman and Vail (1999) (Fig. 11). The main uncertainties that could derive from applying this methodology arise from an erroneous seismic interpretation and/or depth conversion, and the inability of the numerical modelling tool to accurately estimate crustal stretching (Wenke, 2014). The model shows that the Early Jurassic was characterized by a relatively high sediment flux to the basin (Fig 11) which decreased gradually during the Middle and Late Jurassic (note that the peak at 165 Ma occurs at the shelf and should not be extrapolated to the salt basin). This high sediment flux correlates with high regional subsidence rates related to the thermal subsidence stage which particularly affected the PAD. From the Middle to Late Jurassic, high sedimentation rates related to carbonate platform aggradation took place at the Tarfaya Basin shelf region (Figs. 11). However, the salt basin was not affected by this fast aggradation and its related loading effect since the platforms were located updip from the proximal salt pinch-out (Figs. 4a and "Tithonian Slope Break" on 9a). We submit that the large thickness variations (ranging from 500 m to more than 3500 m) observed in the PAD (Fig. 9a) during this stage are related to local early minibasin subsidence.

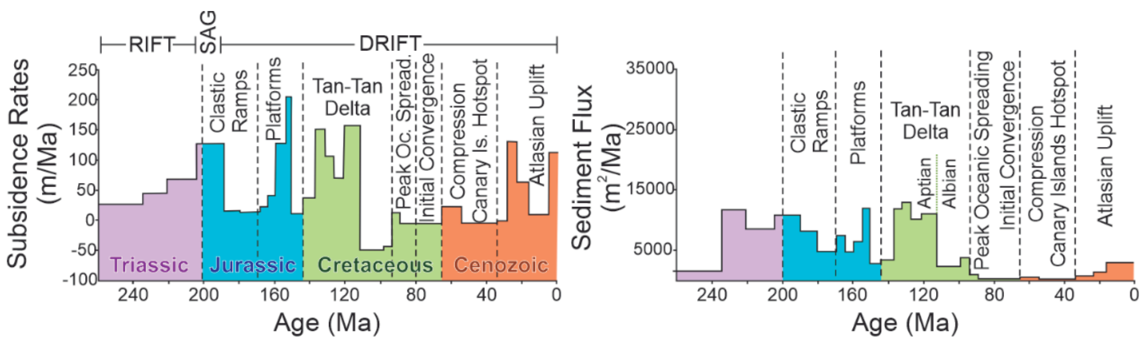

Figure 11. Subsidence rates and total sediment flux redrafted from Wenke (2014) for the offshore Tarfaya Basin from a transect located close to seismic transect A-A' (Tan-Tan transect in Fig. 3)

The base of the Cretaceous is marked by an unconformity recording the erosion of the Upper Jurassic shelf carbonates (MDU in Fig. 2) (Ranke, et al., 1982). The erosional character of this unconformity is clearly observable in the proximal domain (Fig. 4a), whereas it evolves into a correlative conformity basinward. Overlying this surface is a thick (up to 4 km) Lower Cretaceous prograding sequence as observed in figures 4a and 9b. Regional seismic interpretation combined with onshore stratigraphy and well correlation allow to assign these sediments to the distal facies of the Tan-Tan Delta (Martinis and Visintin, 1966; Ratschiller, 1970; Ranke et al., 1982; El Khatib and Ruellan, 1995; Wenke, 2014; Gouiza et al., 2017) exposed at the onshore Tarfaya Basin (Fig. 1).

Figure 11 shows high subsidence and sediment flux rates related to the Tan-Tan Delta from Berriasian to Aptian times. The thickness distribution of the sediments derived from the delta is shown in Figure 9b. Maximum thickness is observed at the proximal (shelf break/slope), central and northeastern areas of the PAD. The Lower Cretaceous interval is thinner in the southwest (1 to 2.5 km) and especially on the CJH, where thickness is less than 1 km (Fig. 9b).

The BCU can be clearly identified on all the presented seismic transects. The most prominent basal truncations against the BCU are observed at the shelf and slope regions. These basal truncations are restricted to the Aptian to Upper Cretaceous interval (Figs. 4, 6 and 8) except for profile E-E' (Fig. 7) where the truncated interval includes the Valanginian/Hauterivian to Upper Cretaceous succession. In distal settings, the angularity between Cretaceous strata and the BCU progressively diminishes, eventually becoming a correlative conformity at the distal end of the basin. In this area, the limit between the Cretaceous and the Cenozoic is identified by a set of high amplitude reflectors (Fig. 4a), with Cenozoic reflectors onlapping against the BCU. Volcanic rocks are interpreted in the most distal region of the PAD (Figs. 4a and 7). These bodies are characterized by strong reflectivity and discontinuous seismic character. In general, they are concordant with the Cenozoic strata, although, in some cases, intrusive bodies are also noticeable at Mesozoic levels (Fig. 7). In general, Oligocene reflectors onlap most of these volcanic bodies suggesting they have an extrusive origin.

5 Interpretation and discussion

5.1 Role of inheritance and paleo-topography (Triassic – Early Jurassic)

The early evolution of the Tarfaya Basin was influenced by the inherited Variscan structures controlling the location and geometry of the Triassic extensional system (Le Roy and Piqué, 2001) (Figs. 12a and 13a). The southern boundary of the basin corresponds to the transition from a northern magma-poor to a southern magma-rich passive margin, as defined by Louden et al. (2013) in the southern Nova Scotia conjugate margin. As pointed out by Rowan (2014), this transition could imply the presence of a topographic high due to excess heat and uplift associated with the magmatic event, that may inhibit the development of a salt basin, providing the barrier that isolated the salt basin from the world ocean to the south (earlier spreading to the S), as is the case in the Pelotas to Santos Basin transition, in the South Atlantic offshore Brazil (Stica et al., 2014).

Figure 12 shows a four-step structural restoration of a simplified version of seismic transect A-A' (Fig. 4a). As can be noticed on the "Top Salt" stage (Hettangian-Sinemurian) (Fig. 12a), the CJH constituted a subtle, broad paleo-high during salt deposition. Initially, the salt layer was deposited with a wedge-shaped geometry, with the thickest accumulation at the distal western boundary of the PAD and progressively thinning eastward. The maximum salt thickness estimated through sequential restoration (Rowan, 1993) at this stage is of ca. 2.0 km adjacent to the basement step-up onto the outer high, with a top salt slope angle of 1.3º and a relative maximum depth to the top of salt of 2.5 km (Fig. 12a). The absolute basin and brine depths are unknown. Salt deposition was concomitant with a higher accommodation space in the PAD compared to the more proximal Tan-Tan and Tarfaya depocenters. This is explained by the basinward shifting of crustal faulting model proposed by Le Roy and Pique (2001), being the PAD the last to subside. At the same time, crustal thinning provided most of the subsidence required for salt to be deposited in the PAD while Cap Juby High acted as a paleo-high (Necking Domain) (Fig. 12a) constraining salt deposition. This evaporitic depositional setting is analogous to other well-known late syn-rift to post rift salt basins in the world as the Gulf of Mexico or the South Atlantic (Hudec and Peel, 2019; Rowan, 2020a; Rowan, in press).

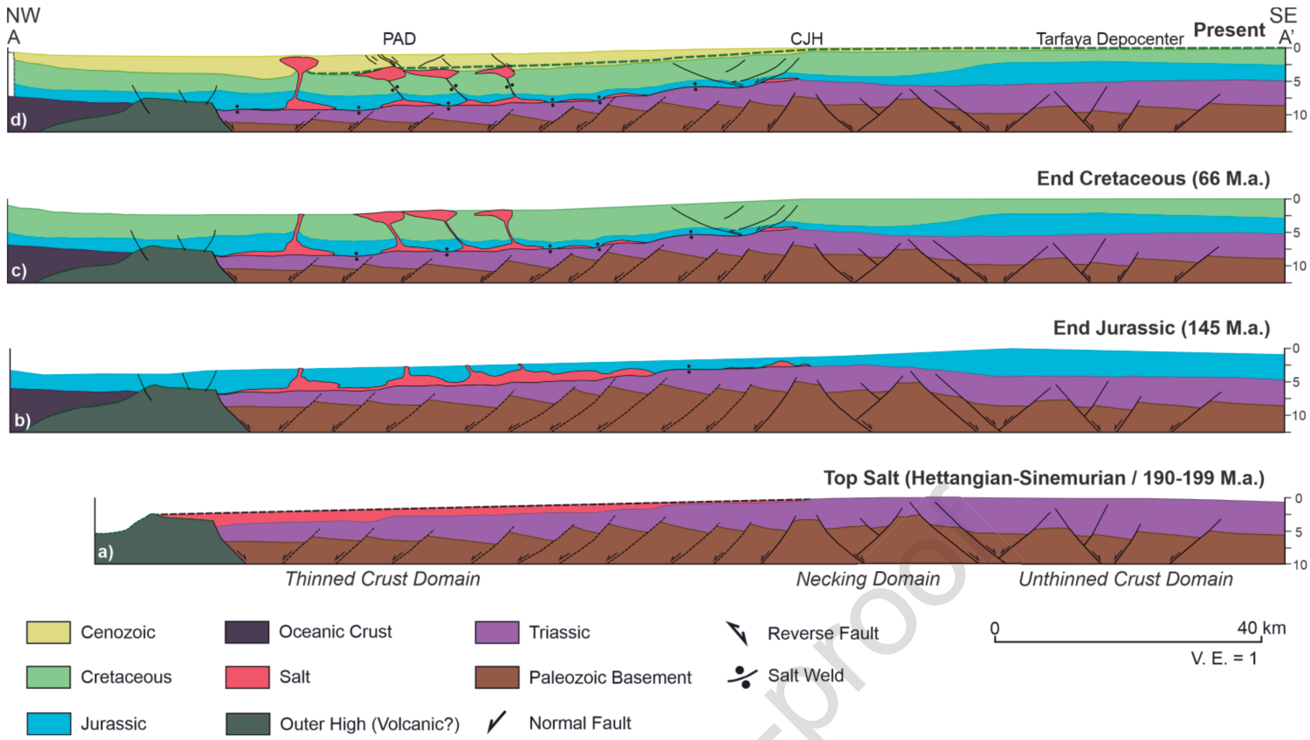

Figure 12. Sequential structural restoration of a simplified version of seismic transect A-A' (Fig. 4a), following methodology introduced by Rowan (1993) that incorporates decompaction, calculation of paleo-water depth, thermal and isostatic subsidence. The black dashed line marking the top of salt on a) represents the hypothetical maximum salt thickness possible. The actual initial salt thickness is uncertain. Dark-green dashed line on d) represents the estimated Upper Cretaceous thickness before the Base Cenozoic erosional unconformity.

The nature of the crust underlying the western border of the Tarfaya Basin PAD is uncertain since no well has penetrated it and geophysical data allow ambiguous interpretations (Roesser et al., 2002; Contrucci et al., 2004; Minshull 2008; Biari et al., 2015; Klingelhoefer et al., 2016). The presence of highly reflective volcanic rocks related to the evolution of Fuerteventura and Lanzarote Islands significantly hinders seismic imaging. However, some first-order interpretations can be made relying on selected seismic profiles (for example, profile A-A' in Fig. 4a). The PAD is developed over thinned continental crust in a distal passive margin setting between the crustal necking and the oceanic crust domains, as defined by Peron-Pinvidic et al. (2017). This distal domain includes a hyper-extended subdomain which may contain an outer high as the one observed in figures 4a, 7 and 12a. However, no conclusive evidence regarding the nature of this high exists, only a step or abrupt change in basement structural relief (see Tugend et al., 2015; Rowan, 2018).

Outer highs are common features present in the distal domain of rifted passive margins like the Santos Basin (Mohriak, et al., 2008), Gulf of Mexico (Rowan, 2018), the Vøring Basin (Gernigon et al., 2003) or offshore

Gabon (Epin et al., 2021), amongst others. These features are frequently observed in seismic, gravity and magnetic data but have been scarcely drilled (Manatschal, et al., 2010). As a result, their origin and composition are highly uncertain in most cases. The most common proposed origins for these features can be grouped in four different classes: basement allochthons over the hyperextended domain, exhumed mantle, oceanic/proto-oceanic crust, magmatic underplating/volcanic high. These are only end-member classifications and different combinations between them can coexist (Tugend, et al., 2018; Sapin, et al., 2021). In general, basement allochthons display overlapping sedimentary wedges that record the rotation of the faulted block as it was transported (Peron-Pinvidic et al., 2013) whereas exhumed mantle is commonly structured at 9 to 10 s TWT (in the absence of dynamic topography or loading) and shows no internal reflectivity (Peron-Pinvidic et al., 2013). In the PAD, no diagnostic features corresponding to a basement allochthon or exhumed mantle origin are observed. This leaves only two possibilities left: an oceanic/proto-oceanic or a magmatic underplating/volcanic origin.

Some distinguishable observed features in the distal domain of the PAD are a change in seismic facies (from more continuous to chaotic to the west) and a step up in basement morphology (Fig. 4a and 7). Also, as interpreted on profile A-A' (Fig. 4a), the top of the oceanic crust is located stratigraphically higher and westward from the distal pinch-out of the autochthonous salt, which coincides approximately with the S1 magnetic anomaly (Roesser et al., 2002). This is also confirmed by refraction and wide-angle seismic reflection profiles from the northern Moroccan margin (Klingelhoefer et al., 2016). Moreover, following Louden et al. (2012), it can be argued that the Tarfaya Basin is located within the transition between a magma poor and magma rich margin. In addition, some disruptive, high amplitude seismic reflections characteristic of intrusive bodies are observed overlying the outer high in profile E-E' (Fig. 7). All these evidences suggest that the outer high may have a magmatic/volcanic origin. Accordingly, the outer high would predate or at most have been synchronous with salt deposition since it acted as a distal barrier during this stage (Fig. 12a and 13a). In this context, and following criteria proposed by Rowan (2014), salt deposited in the Tarfaya Basin should be classified as syn-thinning.

In the Essaouira Basin (Fig. 1), salt thickness correlates with syn-rift faults (Hafid et al., 2000; Hafid et al., 2006; Tari et al., 2017) whereas in the Tarfaya Basin most of the faults do not offset salt (Figs. 4a, 7 and 8). Conceptually, this could be a consequence of either diachronous deposition of salt along the Moroccan margin or a synchronous salt deposition during the "unzipper" (after Schettino and Turco, 2009 in Rowan, 2014) opening propagation of the Morocco-Nova Scotia conjugate margins which gets younger to the north (Le Roy and Piqué, 2001; Schettino and Turco, 2011), allowing syn-thinning salt to be deposited in the thinned distal domain in the southern Tarfaya Basin (post-tectonic) whereas, at the same time, it may have been deposited in the necking or unthinned domain in the northern Essaouira Basin (syn-tectonic).

5.2 Early-stage salt tectonics (Early to Late Jurassic)

The high subsidence rates calculated for the thinning stage (Fig. 11), particularly in the PAD (Wenke, 2014), caused basinward tilting of the basin. Structural restoration of seismic transect A-A' shows an increase in slope gradient from 1.3º (Fig. 12a) to 1.7º (Fig. 12b), with relative restored depths to the Top Jurassic of 3.3 km at the distal boundary of the PAD.

Proximal extension and gravity gliding due to regional tilting during the thermal subsidence stage have been well documented on other salt-bearing basins as being main driving mechanisms for salt mobilisation (e.g., Nova Scotia, Angola, NE Greenland, Brazil, NW Mediterranean, among others) (Deptuck and Kendell, 2017; Hudec and Jackson, 2004; Rowan et al., 2012; Davison, 2007; Granado et al., 2016, respectively). However, even though there are some evidences of incipient gravity gliding in the proximal domain of the Tarfaya Basin (Figs. 4a and 7), these are scarce, local and with no correlative early contractional deformation observed in distal areas. Furthermore, as observed on profiles A-A' (Fig. 4a) and E-E' (Fig. 7), this incipient basement-detached system took place at a later stage of basin evolution (Early Cretaceous), so gravity gliding must be discarded as a main trigger for salt mobilization. Gravity gliding requires enough dip of the top salt over a layer with a high longitude (L) / thickness (H) ratio of the overburden (Rowan et al., 2012; Lehner and Schöpfer, 2018). For a slope angle of 1º (close enough to the 1.3º slope measured through structural restoration on profile A-A', see Fig. 12a), a L/H ratio of 75 is required to trigger gravity gliding (Lehner and

Schöpfer, 2018). The salt basin on profile A-A' is ~70 km wide, meaning it would be near the theoretical limit only when the overburden was ~1 km thick. Moreover, the calculated theoretical value of 75 is considered for normal-strength siliciclastics, whereas carbonate rocks tend to cement very quickly and are therefore stronger, implying that a higher dip and/or longer distance is required for failure. Thus, the initial conditions for gravity gliding did not took place in the PAD due to an insufficient lateral gradient in elevation head. Another factor that might have hampered early gravity gliding is the possibility that salt was removed from the higher proximal areas by downslope drainage as proposed for other passive margins (Davison et al., 2012; Quirk et al., 2012).

Gravity spreading (Nye, 1952; Ramberg, 1981b; Ge et al., 1997) caused by the agrading Jurassic carbonate platform appears unlikely to have triggered salt tectonics since the basinward edge of the platform was located landward from the proximal salt pinch-out (Fig. 4a and the "Tithonian Slope Break" on Fig. 9a). However, the seismic interpretation shows that expulsion rollovers (Fig. 6a, east of Cap Juby High and MO-3 well) and, to a lesser degree, turtle back structures (Fig. 4a) started to develop in proximal areas during the Early Jurassic. Furthermore, the general trend of basinward-migrating depocenters observed on almost all seismic transects and the Jurassic thickness map (Fig. 9a) shows thick proximal minibasins suggesting that salt withdrawal was a strong driver providing accommodation space for the incoming sediments sourced from the Reguibat Shield and, to a lesser extent, from the Western Anti Atlas (Leprêtre et al., 2015; Gouiza et al., 2017; Charton et al., 2021a). At proximal areas within the PAD, these early local depocenters progressively shifted basinward leading to the growth of basinward-leaning diapirs (Figs. 9b and 12b). As pointed out by Rowan (2017), these diapirs are typically developed at the paleo-slope region. Therefore, we infer that the progradational loading of the Early Jurassic paleo-slope, basinward from the platform edge and over the proximal part of the salt basin, likely triggered initial gravity spreading and the onset of salt mobilisation in the central and northern areas of the Tarfaya Basin (Fig. 13b).

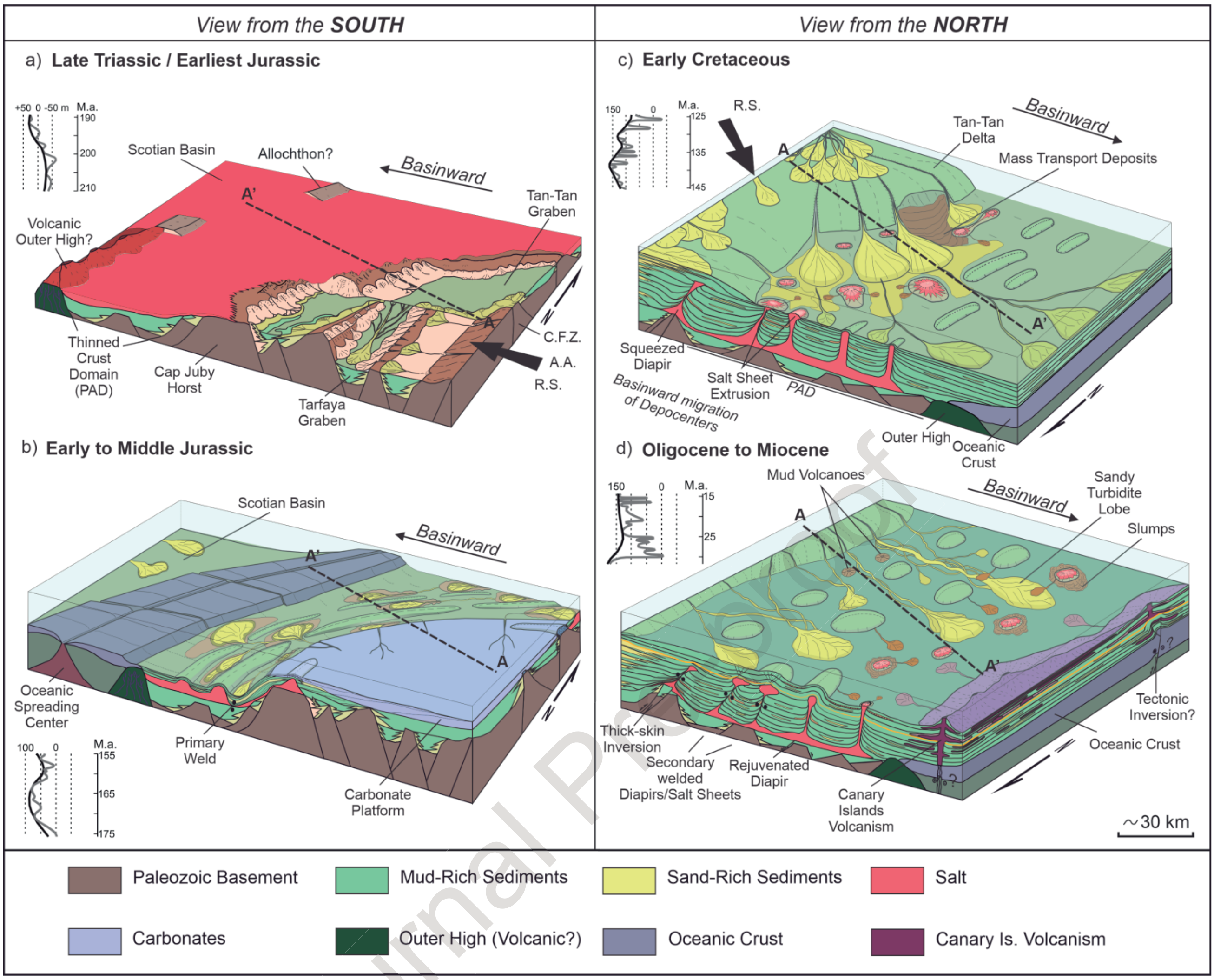

Figure 13. 3D conceptual model for the evolution of the Tarfaya Basin. a) and b) show a perspective view from the south, whereas c) and d) show a perspective view from the North. Seismic transect A-A' is used only as a location reference. Global eustatic sea level curves from Haq et al., 1987; **a)** Rift-Drift transition stage; A.A.: Anti Atlas; R.S.: Reguibat Shield (Gouiza, et al., 2017; Charton et al., 2021a); **b)** Onset of seafloor spreading (Toarcian?); **c)** Progradation of the Tan-Tan Delta (Berriasian to Albian). Sediment provenance mainly from the R.S. (Ali, et al., 2014; Charton, et al., 2021a) and minor contributions from the Western Anti Atlas (Arantegui, et al., 2019). Channelization in sediment routing influenced by salt structures as described in the onshore Essaouira Basin (Charton, et al., 2021b) **d)** Effects of shortening. Distal volcanism from the eastern Canary Islands. See section 4 for explanation.

Although expulsion rollovers and counterregional welds are common in proximal areas, the most distal diapirs and those near the southwestern border of the PAD have vertical stems and more vertically stacked depocenters (Fig. 9b) that include Early Jurassic minibasins. It is not clear what factors triggered and controlled the distribution of these early depocenters located distally from the paleo-slope. It is possible that cryptic and undocumented small amounts of gravity gliding related with post-rift thermal subsidence and hinterland uplift may have been responsible for setting up early minor highs and lows that conditioned subsequent feedback and the initiation of diapirism and minibasin subsidence.

5.3 Tan-Tan Delta progradation (Early Cretaceous – Late Cretaceous)

The Tan-Tan Delta progradation further promoted the progressive basinward expulsion of salt, as evidenced by the continued basinward migration of depocenters (expulsion-rollover structures; Ge et al., 1997) and the seaward-leaning stems during the Early Cretaceous (best exemplified on Figs. 4a, 6a and 7). On the proximal fringe of salt structures, lateral salt emplacement initiated during the Barremian-Aptian interval (Figs. 10 and 12c), likely promoted by a gradual increase in the ratio between salt-supply and sediment-accumulation rates. As pointed out by Hudec and Jackson (2006), the basal cutoffs of salt against sequentially younger beds can be used to trace the growth history of salt sheets in map view. Following their criteria, the decrease in sedimentation rates recorded during the Late Cretaceous (Fig. 11) could have accelerated the lateral emplacement of the salt sheets (Fig. 10). Moreover, former seaward-leaning feeders (Fig. 13c) evolved into counterregional secondary welds separating asymmetric basinward-dipping minibasins (Fig. 4a) (for examples see Rowan and Inman, 2005). As can be observed in Fig. 9b, this system of counterregional welded feeders tends to match with areas having the thickest Lower Cretaceous sedimentary accumulations indicating it was fostered by the relatively steep slope gradient of the prograding Tan-Tan Delta (Fig. 13c), as it is the case in the northern Gulf of Mexico and the Scotian margin (Rowan, 2017). In contrast, the more distal fringe of vertical open feeders (Fig. 9b) probably formed basinward of the Early Cretaceous toe-of-slope.

Along strike differences in sedimentary thickness (Fig. 9b) during the progradation of the Tan-Tan Delta had an additional impact on salt tectonics. In the northern region of the Tarfaya Basin, with a thicker Lower Cretaceous succession, the pressure-head gradient caused by the progradational loading promoted minor gravity spreading (Schultz-Ela, 2001; Rowan, et al, 2004; Vendeville, 2005) in a basinward direction, triggering a local salt-detached linked system of proximal extension and downdip contraction. This deformation was restricted to a specific area (only observed on seismic transects A-A' and E-E'; Figs. 4a and 7, respectively) and did not affect areas where the Lower Cretaceous succession was thinner. Interpreted growth strata constrain this event between Berriasian and Aptian times. Simultaneously, the more distal passive diapirs kept growing driven by sedimentary loading and evacuation of the salt beneath the surrounding minibasins (Fig. 13c).

5.4 Late shortening (Late Cretaceous – Quaternary)

Low-temperature thermochronological and regional studies indicate that an exhumation stage took place in the hinterlands of the Tarfaya Basin during the Late Cretaceous (Guiraud and Bosworth, 1997; Frizon de Lamotte et al., 2009; Sehrt, 2014; Leprêtre et al., 2015; Gouiza et al., 2017; Charton et al., 2021a), pointing to the initial convergence between Africa and Eurasia as the main cause (Hafid et al., 2008; Neumaier et al., 2016). Moreover, Tari and Jabour (2013) proposed tectonic inversion as one of the mechanisms driving salt sheet extrusion during the Cenozoic in the neighboring Essaouira Basin. Shortening of salt structures on passive margins may be the result of gravitational failure (Hudec and Jackson, 2004; Rowan et al., 2012; Deptuck and Kendell, 2017, amongst others). However, gravity spreading or gliding cannot explain the shortening observed in the Cenozoic (Fig. 12d). First, no evidence for a salt-detached system exists during this period, since no Cenozoic updip extension is observed along the salt basin. Second, there is no salt weld or detachment that would link hypothetical updip extension to downdip contraction. Moreover, no gravity-driven deformation can explain the prominent folded Triassic strata and the inverted Paleozoic basement blocks observed on seismic transects E-E' and F-F' (Figs. 7 and 8). Therefore, the Late Cretaceous and Cenozoic contraction is attributed to the orogenic shortening caused by the convergence between Africa and Iberia (Guiraud and Bosworth, 1997; Frizon de Lamotte et al., 2009; Neumaier et al., 2016).

The orogenic event caused thick-skinned inversion in the Tarfaya Basin (Fig. 13d), a process evident on the eastern basement blocks delimiting the CJH and its northern extension (Figs. 6, 7 and 8). There are no indications, however, of a direct connection between crustal shortening structures and suprasalt deformation. This can be explained by the fact that salt can decouple deformation without a hard ramp-flat transition, as is the case in central Poland where the locations of presalt and suprasalt deformation were separated by 30-40 km along the stress direction (Rowan and Krzywiec, 2014). At the margin scale, shortening subsequently led to the erosion of much of the Upper Cretaceous succession (BCU) at the shelf and slope regions (Michard, 1976; Uchupi et al., 1976; Sehrt, 2014; Leprêtre et al., 2015; Gouiza et al., 2017).

Shortening probably accelerated the lateral emplacement of salt sheets (Figs. 4a, 6, 7 and 8). Moreover, there was also a marked decrease in sediment-flux rates during Late Cretaceous times (Fig. 11) due to a global sea level rise and increased subsidence / low exhumation rates in the hinterland of the Tarfaya Basin (Wenke, 2014; Charton et al., 2021a), further promoting salt-sheet advance. Overall, the combined effects of these processes (thick-skinned shortening and decrease in sedimentation rates) caused an increase in lateral emplacement rates and contributed to the squeezing of diapirs stems (already affected by sediment progradation), which eventually led to secondary welding in the proximal domain.

Basinwide, two distinctive types of late salt deformation can be interpreted: proximal salt structures with thick Cenozoic pre-arching roofs (above regional) and distal diapirs with thinner roofs actively deforming the seabed (Fig. 9c). Distal structures display intervals of truncating strata against their flanks (passive stage) followed by intervals showing basal truncations of pre-arching strata against syn- to post-arching strata (for example, see distal diapir #5 on Fig. 7). This suggests that these long-lived salt structures have been rejuvenated (Vendeville and Nilsen, 1995) several times during the Cenozoic (Fig. 12d). Proximal salt sheets were also rejuvenated by shortening, as evidenced by erosional truncations of thick pre-arching roofs and onlapping Pliocene strata (Fig. 4a). Most of these more proximal salt structures were rejuvenated during Neogene times after their feeders and/or the authochtonous salt were welded, whereas the distal fringe of diapirs and salt sheets continue actively growing to the present (Fig. 13d), actively deforming the seabed. Active growth in these structures is possible due to the presence of open stems and ongoing salt withdrawal from distal minibasins (Fig. 9c). As shown on the structural restoration (Fig. 12), the initial wedge-shaped geometry of the salt basin, with the thickest accumulation in the most distal area, allowed for a continuous supply of salt to these distal structures. At the same time, the proximal salt stuctures were already welded.

5.5 Comparison with other late syn-rift/syn-thinning salt basins

As observed through the presented seismic profiles, gravity-driven deformation is minimal in the offshore Tarfaya Basin. A typical reason for this is the timing of evaporite deposition relative to rifting. Early syn-rift basins have little/no such deformation (e.g., Iberia/Newfoundland, Barents Sea, NE Greenland) (Alves et al., 2006; Rowan and Lindsø, 2017) whereas, in general, mid to late syn-rift basins exhibit large amounts of gravity-driven deformation (e.g., Gulf of Mexico, South Atlantic) (Davison, 2007; Rowan, 2020b; amongst others). However, the Tarfaya Basin constitutes an exception to the common structural styles described for late syn-rift basins. As discussed in section 5.2, the most likely cause is the narrowness of the salt-bearing depocenter (PAD).

North of the Tarfaya Basin, the Agadir segment of the EAB shows a wider salt basin characterized by isolated diapirs evolving to a distal toe-thrust anticline (see figure 6.10c in Hafid et al., 2008). Interestingly, these diapirs are actively deforming the seabed in both proximal and distal locations, in contrast to the Tarfaya Basin where only distal structures deform the seafloor (Figure 9c). This could be related to different initial salt thickness distributions between the two basins. The original salt layer in Agadir might have had a more tabular shape than the initial wedge-shaped geometry described for the offshore Tarfaya Basin (Figure 12a). Furthermore, no salt sheets or canopies are described in the Agadir segment, possibly due to a lack of sufficient progradational loading from the Tan Tan Delta (see the line corresponding to the shoreline position of the Tan Tan Delta in Figure 1).

Northward, the Essaouira segment of the EAB and the Safi basin display proximal rafts and turtles evolving basinward to canopies and tongues and a prominent distal toe-thrust system (Tari et al., 2000; Tari et al., 2003; Tari and Jabour, 2013). This structural style relates to an increase in the width of the salt basin and its general basinward dipping attitude. Furthermore, the closeness of this region to the Atlas System promoted major thick-skinned inversion in the proximal domain since Late Cretaceous times (Hafid et al., 2006; Neumaier et al., 2016; Pichel et al., 2019). This contractional event had a more pronounced effect on the structural style of the Essaouira and Safi basins than that of the Tarfaya Basin.

6 Conclusions

This study has presented unpublished 2D and 3D seismic data calibrated with wells from the offshore Tarfaya Basin. Through a detailed seismic interpretation workflow and sequential restoration, it was possible to build up a solid tectonostratigraphic framework to characterize the main controlling factors that influenced the salt basin evolution.

Salt was deposited on a narrow rifted margin over thinned continental crust during the syn-thinning stage. The western boundary of the basin is a basement step up at the continent-ocean transition which we interpret as a volcanic outer high. The Cap Juby High constituted a paleo-high which acted as a threshold constraining salt distribution and thickness to the east. Salt was deposited between Late Triassic and Early Jurassic times with a wedge-shaped geometry and a maximum thickness at the western distal margin and progressively thinning to the east. The evaporite basin was split in two by oceanic spreading, with the other half now on the conjugate Scotian margin.

During the Jurassic, local depocenters and related salt withdrawal were probably triggered by progradational loading on the demised carbonate slope on a proximal setting. Thermal subsidence might have led to the regional tilting of the salt basin probably playing an important role as triggering mechanism in the distal basin. However, no widespread updip extension and related downdip contraction is observed in the Jurassic interval, probably due to the narrow geometry of the salt basin that hampered gravity gliding.

During the Early Cretaceous, progradation of the Tan-Tan Delta contributed to the already ongoing basinward expulsion of salt. A proximal fringe of seaward-leaning diapirs located at the paleo-slope and a distal fringe of salt structures with nearly vertical stems beyond the paleo toe-of-slope were developed. From Barremian times, the interplay between sediment-accumulation and salt-supply rates led to the emplacement of salt sheets mainly located in the proximal domain of the salt basin. Sediment loading from the Tan-Tan Delta promoted the development of a local salt-detached system of linked extension and contraction.

From Late Cretaceous onwards, shortening related to the convergence between the African and Eurasian plates resulted in thick-skinned inversion, erosion and the rejuvenation of diapirs and salt sheets. Consequently, a proximal fringe of diapirs formed secondary welds whereas distal diapirs and salt sheets continue actively growing, even deforming the modern seabed.

7 Acknowledgments

The authors would like to thank REPSOL for providing the seismic and well data used in this study. This study is part of the first author's doctoral thesis project that has been supported by an APIF grant from the University of Barcelona, by the projects "Tectónica Salina en Cinturones Contractivos" (SALTCONBELT-CGL2017-85532-P), funded by Agencia Estatal de Investigación (AEI) and Fondo Europeo de Desarrollo Regional (FEDER). We acknowledge the support of the research project Structure and Deformation of Salt-bearing Rifted Margins (SABREM), PID2020-117598GB-I00, funded by MCIN/AEI/10.13039/501100011033. Rodolfo Uranga acknowledges the funds from the AAPG's Chandler and Laura Wilhelm Grant and by "Ajuts de borses de viatges per a estudiants del Programa de Doctorat de Ciències de la Terra" from the University of Barcelona and the GEOMODELS Research Institute for scientific discussions and support. Mark Rowan is supported by the Salt-Sediment Interaction Research Consortium at The University of Texas at El Paso. Schlumberger is acknowledged for providing Petrel software, Eliis for providing Paleoscan software and Petroleum Experts for providing Move software. Discussions with Gianreto Manatschal and Leonardo Pichel contributed significantly to this research. The authors deeply thank Gabor Tari and Remi Charton for their constructive reviews and comments that greatly improved the original manuscript.

8 Appendix A. Supplementary Data

Supplementary data to this article can be found online at

References

AbouAli, N., Hafid, M., Chellaï, E. H., Nahim, M., Zizi, M., 2005. Structure de socle, sismostratigraphie et héritage structural au cours du rifting au niveau de la marge d'Ifni/Tan-Tan (Maroc sud-occidental). *Comptes Rendus Geoscience*, *337*(14), 1267-1276. DOI: 10.1016/j.crte.2005.07.003

Allen, J., Beaumont, C., 2016. Continental margin syn-rift salt tectonics at intermediate width margins. Basin Research, 28(5), 598-633. DOI: 10.1111/bre.12123

Ali, S., Stattegger, K., Garbe-Schönberg, D., Frank, M., Kraft, S., Kuhnt, W., 2014. The provenance of Cretaceous to Quaternary sediments in the Tarfaya basin, SW Morocco: Evidence from trace element geochemistry and radiogenic Nd–Sr isotopes. *Journal of African Earth Sciences*, *90*, 64-76. DOI: 10.1016/j.jafrearsci.2013.11.010

Alves, T. M., Moita, C., Sandnes, F., Cunha, T., Monteiro, J. H., Pinheiro, L. M., 2006. Mesozoic–Cenozoic evolution of North Atlantic continental-slope basins: The Peniche basin, western Iberian margin. *AAPG bulletin*, *90*(1), 31-60.

Ancochea, E., Huertas, M. J., 2003. Age and composition of the Amanay seamount, Canary Islands. Marine Geophysical Research, 24(1), 161-169. DOI: 10.1007/s11001-004-1100-7

Anguita, F., Hernán, F., 2000. The Canary Islands origin: a unifying model. Journal of Volcanology and Geothermal Research, 103(1-4), 1-26. DOI: 10.1016/S0377-0273(00)00195-5

Arantegui, A. I., 2019. *Characterisation of Mesozoic Depositional Systems along the Atlantic Passive Margin of Morocco. North Aaiun-Tarfaya Basin* (Doctoral dissertation, The University of Manchester, United Kingdom).

Biari, Y., Klingelhoefer, F., Sahabi, M., Aslanian, D., Schnurle, P., Berglar, K., Reichert, C., 2015. Deep crustal structure of the north-west African margin from combined wide-angle and reflection seismic data (MIRROR seismic survey). Tectonophysics, 656, 154-174. DOI: 10.1016/j.tecto.2015.06.019

Biari, Y., Klingelhoefer, F., Sahabi, M., Funck, T., Benabdellouahed, M., Schnabel, M., Reichert, C., Gutscher, M. A., Bronner, A., Austin, J. A., 2017. Opening of the central Atlantic Ocean: implications for geometric rifting and asymmetric initial seafloor spreading after continental breakup. *Tectonics*, *36*(6), 1129-1150.

Blackburn, T. J., Olsen, P. E., Bowring, S. A., McLean, N. M., Kent, D. V., Puffer, J., Et-Touhami, M., 2013. Zircon U-Pb geochronology links the end-Triassic extinction with the Central Atlantic Magmatic Province. Science, 340(6135), 941-945. DOI: 10.1126/science.1234204

Blanco-Montenegro, I., Montesinos, F. G., Arnoso, J., 2018. Aeromagnetic anomalies reveal the link between magmatism and tectonics during the early formation of the Canary Islands. Scientific reports, 8(1), 1-14. DOI: 10.1038/s41598-017-18813-w

Bowman, S. A., Vail, P. R., 1999. Interpreting the stratigraphy of the Baltimore Canyon section, offshore New Jersey with PHIL, a stratigraphic simulator. In *Harbaugh, J. W., Watney, W. L., Rankey, E. C., Slingerland, R., Goldstein, R. H., Franseen, E. K. (eds.) Numerical experiments in stratigraphy: Recent advances in stratigraphic and sedimentologic computer simulations.* SEPM SPECIAL PUBLICATION. DOI: 10.2110/pec.99.62.0117

Broughton, P., Trepaniéré, A., 1993. Hydrocarbon Generation in the Essaouira Basin. AAPG Bulletin, 77(6), 999-1015. DOI: 10.1306/BDFF8DC6-1718-11D7-8645000102C1865D

Bulhões, É. M., de Amorim, W. N., 2005. Princípio da SismoCamada Elementar e sua aplicação à Técnica Volume de Amplitudes (tecVA). In *9th International Congress of the Brazilian Geophysical Society* (pp. cp-160). European Association of Geoscientists & Engineers. DOI: 10.1190/sbgf2005-275

Carbó, A., Muñoz-Martín, A., Llanes, P., Álvarez, J., EEZ Working Group, 2005. Gravity analysis offshore the Canary Islands from a systematic survey. In *Geophysics of the Canary Islands* (pp. 113-127). Springer, Dordrecht. DOI: 10.1007/s11001-004-1336-2

Catalán, M., Davila, J. M., ZEE Working Group, 2005. A magnetic anomaly study offshore the Canary Archipelago. In *Geophysics of the Canary Islands* (pp. 129-148). Springer, Dordrecht. DOI: 10.1007/s11001-004-5442-y

Carracedo, J. C., Day, S., Guillou, H., Badiola, E. R., Canas, J. A., Torrado, F. P., 1998. Hotspot volcanism close to a passive continental margin: the Canary Islands. *Geological Magazine*, *135*(5), 591-604. DOI: 10.1017/S0016756898001447

Charton, R., Bertotti, G., Arnould, A. D., Storms, J. E., Redfern, J., 2021a. Low-temperature thermochronology as a control on vertical movements for semi-quantitative source-to-sink analysis: A case study for the Permian to Neogene of Morocco and surroundings. Basin Research, 33(2), 1337-1383. DOI: 10.1111/bre.12517

Charton, R., Kluge, C., Fernández-Blanco, D., Duval-Arnould, A., Bryers, O., Redfern, J., Bertotti, G., 2021b. Syn-depositional Mesozoic siliciclastic pathways on the Moroccan Atlantic margin linked to evaporite mobilisation. *Marine and Petroleum Geology*, *128*, 105018. DOI: 10.1016/j.marpetgeo.2021.105018

Contrucci, I., Klingelhöfer, F., Perrot, J., Bartolomé, R., Gutscher, M. A., Sahabi, M., Rehault, J. P., 2004. The crustal structure of the NW Moroccan continental margin from wide-angle and reflection seismic data. *Geophysical Journal International*, *159*(1), 117-128. DOI: 10.1111/j.1365-246X.2004.02391.x

Curry, M. A., Peel, F. J., Hudec, M. R., Norton, I. O., 2018. Extensional models for the development of passive-margin salt basins, with application to the Gulf of Mexico. *Basin Research*, *30*(6), 1180-1199. DOI: 10.1111/bre.12299

Davison, I., 2005. Central Atlantic margin basins of North West Africa: geology and hydrocarbon potential (Morocco to Guinea). *Journal of African Earth Sciences*, *43*(1-3), 254-274. DOI: 10.1016/j.jafrearsci.2005.07.018

Davison, I., 2007. Geology and tectonics of the South Atlantic Brazilian salt basins. *Geological Society, London, Special Publications*, *272*(1), 345-359. DOI: 10.1144/GSL.SP.2007.272.01.18

Davison, I., Anderson, L., Nuttall, P., 2012. Salt deposition, loading and gravity drainage in the Campos and Santos salt basins. *Geological Society, London, Special Publications*, *363*(1), 159-174.

Deptuck, M. E., Kendell, K. L., 2017. A review of Mesozoic-Cenozoic salt tectonics along the Scotian margin, eastern Canada. *Permo-Triassic Salt Provinces of Europe, North Africa and the Atlantic Margins*, 287-312.

Deptuck, M.E., 2020. Nova Scotia's volcanic passive margin - exploration history, geology, and play concepts off southwestern Nova Scotia. Canada-Nova Scotia Offshore Petroleum Board, Geoscience Open File Report 2020-001MF, 32p.

Dillon, W. P., 1974. Structure and development of the southern Moroccan continental shelf. Marine Geology, 16(3), 121-143.

El Khatib, J., Ruellan, E., 1995. *Etude structurale et stratigraphique d'un segment de la marge continentale atlantique sud-marocaine: le bassin de tarfaya-laayoune* (Doctoral dissertation, Nice).

Ferrer, O., Gratacós, O., Roca, E., Muñoz, J. A., 2017. Modeling the interaction between presalt seamounts and gravitational failure in salt-bearing passive margins: The Messinian case in the northwestern Mediterranean Basin. Interpretation, 5(1), SD99-SD117. DOI: 10.1190/INT-2016-0096.1

Frizon de Lamotte, D., Saint Bezar, B., Bracène, R., Mercier, E., 2000. The two main steps of the Atlas building and geodynamics of the western Mediterranean. *Tectonics*, *19*(4), 740-761. DOI: 10.1029/2000TC900003

Frizon de Lamotte, D. F., Leturmy, P., Missenard, Y., Khomsi, S., Ruiz, G., Saddiqi, O., Michard, A., 2009. Mesozoic and Cenozoic vertical movements in the Atlas system (Algeria, Morocco, Tunisia): an overview. Tectonophysics, 475(1), 9-28.

Fullea, J., Camacho, A. G., Negredo, A. M., Fernández, J., 2015. The Canary Islands hot spot: New insights from 3D coupled geophysical–petrological modelling of the lithosphere and uppermost mantle. *Earth and Planetary Science Letters*, *409*, 71-88. DOI: 10.1016/j.epsl.2014.10.038

García del Olmo, L., Mojonero, C. G., Cortes, N. A., 2018. Implications of Sandia-1X well results in the hydrocarbon exploration offshore Morocco. In *AAPG Europe Regional Conference, Global Analogues of the Atlantic Margin*.

Gaullier, V., Vendeville, B. C., 2005. Salt tectonics driven by sediment progradation: Part II—Radial spreading of sedimentary lobes prograding above salt. *AAPG bulletin*, *89*(8), 1081-1089. DOI: 10.1306/03310503064

Ge, H., Jackson, M. P., Vendeville, B. C., 1997. Kinematics and dynamics of salt tectonics driven by progradation. *AAPG bulletin*, *81*(3), 398-423. DOI: 10.1306/522B4361-1727-11D7-8645000102C1865D

Gernigon, L., Ringenbach, J. C., Planke, S., Le Gall, B., Jonquet-Kolstø, H., 2003. Extension, crustal structure and magmatism at the outer Vøring Basin, Norwegian margin. *Journal of the Geological Society*, *160*(2), 197-208. DOI: 10.1144/0016-764902-055

Giles, K. A., Rowan, M. G., 2012. Concepts in halokinetic-sequence deformation and stratigraphy. Geological Society, London, Special Publications, 363(1), 7-31. DOI: 10.1144/SP363.2

Gouiza, M., Charton, R., Bertotti, G., Andriessen, P., Storms, J. E. A., 2017. Post-Variscan evolution of the Anti-Atlas belt of Morocco constrained from low-temperature geochronology. *International Journal of Earth* Sciences, 106(2), 593-616. DOI: 10.1007/s00531-016-1325-0

Granado, P., Urgeles, R., Sabat, F., Albert-Villanueva, E., Roca, E., Munoz, J. A., et al, 2016. Geodynamical framework and hydrocarbon plays of a salt giant: the NW Mediterranean Basin. *Petroleum Geoscience*, *22*(4), 309–321. DOI: 10.1144/petgeo2015-084

Guiraud, R., Bosworth, W., 1997. Senonian basin inversion and rejuvenation of rifting in Africa and Arabia: synthesis and implications to plate-scale tectonics. *Tectonophysics*, *282*(1-4), 39-82. DOI: 10.1016/S0040-1951(97)00212-6

Gutiérrez, M., Casillas, R., Fernández, C., Balogh, K., Ahijado, A., Castillo, C., García-Navarro, E., 2006. The submarine volcanic succession of the basal complex of Fuerteventura, Canary Islands: a model of submarine growth and emergence of tectonic volcanic islands. *Geological Society of America Bulletin*, *118*(7-8), 785-804. DOI: 10.1130/B25821.1

Hafid, M., 2000. Triassic–early Liassic extensional systems and their Tertiary inversion, Essaouira Basin (Morocco). *Marine and Petroleum Geology*, *17*(3), 409-429. DOI: 10.1016/S0264-8172(98)00081-6

Hafid, M., Salem, A. A., Bally, A. W., 2000. The western termination of the Jebilet–high Atlas system (offshore Essaouira Basin, Morocco). Marine and Petroleum Geology, 17(3), 431-443. DOI: 10.1016/S0264-8172(98)00082-8

Hafid, M., Zizi, M., Bally, A. W., Salem, A. A., 2006. Structural styles of the western onshore and offshore termination of the High Atlas, Morocco. *Comptes Rendus Geoscience*, *338*(1-2), 50-64. DOI: 10.1016/j.crte.2005.10.007

Hafid, M., Tari, G., Bouhadioui, D., El Moussaid, I., Echarfaoui, H., Aït Salem, A., Nahim, M., Dakki, M., 2008 Atlantic Basins. In: Michard A., Saddiqi O., Chalouan A., Lamotte D.F. (eds) Continental Evolution: The Geology of Morocco. Lecture Notes in Earth Sciences, vol 116. Springer, Berlin, Heidelberg. DOI: 10.1007/978-3-540-77076-3_6

Haq, B. U., Hardenbol, J. A. N., Vail, P. R., 1987. Chronology of fluctuating sea levels since the Triassic. *Science*, *235*(4793), 1156-1167. DOI: 10.1126/science.235.4793.1156

Heyman, M. A. W., 1989. Tectonic and Depositional History of the Moroccan Continental Margin: Chapter 21: European-African Margins. In: Tankard, A. J., & Balkwill, H. R. (eds.) Extensional Tectonics and Stratigraphy of the North Atlantic Margins. AAPG Memoir 46. DOI: 10.1306/M46497C21

Hinz, K., Dostmann, H., Fritsch, J., 1982. The continental margin of Morocco: seismic sequences, structural elements and geological development. In: von Rad U., Hinz K., Sarnthein M., Seibold E. (eds) Geology of the Northwest African Continental Margin (pp. 34-60). Springer, Berlin, Heidelberg.

Holik, J. S., Rabinowitz, P. D., Austin Jr, J. A., 1991. Effects of Canary hotspot volcanism on structure of oceanic crust off Morocco. Journal of Geophysical Research: Solid Earth, 96(B7), 12039-12067. DOI: 10.1029/91JB00709

Hooghvorst, J. J., Harrold, T. W., Nikolinakou, M. A., Fernandez, O., Marcuello, A., 2020. Comparison of stresses in 3D v. 2D geomechanical modelling of salt structures in the Tarfaya Basin, West African coast. *Petroleum Geoscience*, *26*(1), 36-49. DOI: 10.1144/petgeo2018-095

Hudec, M. R., Jackson, M. P., 2004. Regional restoration across the Kwanza Basin, Angola: Salt tectonics triggered by repeated uplift of a metastable passive margin. *AAPG bulletin*, *88*(7), 971-990. DOI: 10.1306/02050403061

Hudec, M. R., Jackson, M. P., 2006. Advance of allochthonous salt sheets in passive margins and orogens. *AAPG bulletin*, *90*(10), 1535-1564. DOI: 10.1306/05080605143

Hudec, M. R., Jackson, M. P., 2007. Terra infirma: Understanding salt tectonics. *Earth-Science Reviews*, *82*(1-2), 1-28.

Hudec, M. R., Peel, F. J., 2019. A Critical Review of Models for Deposition of the Louann Salt, and Implications for Gulf of Mexico Evolution. In: Fiduk, J. C., Rosen, N. C. (eds) Salt Tectonics, Associated Processes, and Exploration Potential: Revisited 1989-2019. SEPM 37th Annual Conference.

Jackson, M. P., Hudec, M. R., 2017. *Salt tectonics: Principles and practice*. Cambridge University Press.

Klingelhoefer, F., Labails, C., Cosquer, E., Rouzo, S., Geli, L., Aslanian, D., Olivet J. -L., Sahabi, M., Nouzé, H., Unternehr, P., 2009. Crustal structure of the SW-Moroccan margin from wide-angle and reflection seismic data (the DAKHLA experiment) Part A: Wide-angle seismic models. *Tectonophysics*, *468*(1-4), 63-82. DOI: 10.1016/j.tecto.2008.07.022

Klingelhoefer, F., Biari, Y., Sahabi, M., Aslanian, D., Schnabel, M., Matias, L., Benabdellouahed, M., Funck, T., Gutscher, M., Reichert, C., Austin, J. A., 2016. Crustal structure variations along the NW-African continental margin: a comparison of new and existing models from wide-angle and reflection seismic data. *Tectonophysics*, *674*, 227-252. DOI: 10.1016/j.tecto.2016.02.024

Klitgord, K. D., Schouten, H., 1986. Chapter 22: Plate kinematics of the Central Atlantic. In: Vogt, P. R. & Tucholke, B. E. (eds.) The Geology of North America, Vol. M, The Western North Atlantic Region. The Geological Society of America. DOI: 10.1130/DNAG-GNA-M.351

Labails, C., Olivet, J. L., Aslanian, D., Roest, W. R., 2010. An alternative early opening scenario for the Central Atlantic Ocean. *Earth and Planetary Science Letters*, *297*(3-4), 355-368. DOI: 10.1016/j.epsl.2010.06.024

Lancelot, Y., 1977. The evolution of the central northeastern Atlantic; summary of results of DSDP Leg 41. DOI: 10.2973/dsdp.proc.41.151.1978

Lancelot, Y., Winterer, E. L., 1980. Evolution of the Moroccan oceanic basin and adjacent continental margin - a synthesis. *Initial Reports of the Deep Sea drilling project*, *50*, 801-821.

Lawrence, S., Geoex, S. R. C., 2019. Atlantic Offshore Morocco: New Data, New Insights. *Geoexpro, 16(3), 64-68.*

Lehner, F. K., Schöpfer, M. P., 2018. Slope stability and exact solutions for cohesive critical Coulomb wedges from Mohr diagrams. *Journal of Structural Geology*, *116*, 234-240.

Leprêtre, R., Missenard, Y., Barbarand, J., Gautheron, C., Saddiqi, O., Pinna-Jamme, R., 2015. Postrift history of the eastern central Atlantic passive margin: Insights from the Saharan region of South Morocco. *Journal of Geophysical Research: Solid Earth*, *120*(6), 4645-4666. DOI: 10.1002/2014JB011549

Le Roy, P., Piqué, A., 2001. Triassic–Liassic Western Moroccan synrift basins in relation to the Central Atlantic opening. *Marine Geology*, *172*(3-4), 359-381. DOI: 10.1016/S0025-3227(00)00130-4

Le Roy, P., Pique, A., Le Gall, B., Ait Brahim, L., Morabet, A. M., Demnati, A., 1997. Les bassins cotiers triasico-liasiques du Maroc occidental et la diachronie du rifting intra-continental de l'Atlantique central. *Bulletin de la Société géologique de France*, *168*(5), 637-648.

Lorenz, V., Nicholls, I. A., 1976. The permocarboniferous basin and range province of Europe. An application op plate tectonics. In: *The Continental Permain in Central, West, and South Europe* (pp. 313-342). Springer, Dordrecht.

Louden, K., Wu, Y., Tari, G., 2013. Systematic variations in basement morphology and rifting geometry along the Nova Scotia and Morocco conjugate margins. *Geological Society, London, Special Publications*, *369*(1), 267-287. DOI: 10.1144/SP369.9

Martínez del Olmo, W. M., 2020. The Fúster Casas sedimentary trough (east of the Lanzarote and Fuerteventura Canary Islands, Spain). *Revista de la Sociedad Geológica de España*, *33*(1), 27-42.

Martinis B., Visintin V., 1966. Donnees geologiques sur le basin sedimentaire cotier de Tarfaya (Maroc meridional). In: Reyre D. (ed*.) Sedimentary basins of the African Coasts (symposium): 13-26 Assoc of African Geological Surveys, (Paris)*

Michard, A., 1976. Eléments de géologie marocaine. *Editions du service geologique du Maroc.*

Mohriak, W., Nemčok, M., Enciso, G., 2008. South Atlantic divergent margin evolution: rift-border uplift and salt tectonics in the basins of SE Brazil. *Geological Society, London, Special Publications*, *294*(1), 365-398. DOI: 10.1144/SP294.19

Morabet, A. M., Bouchta, R., Jabour, H., 1998. An overview of the petroleum systems of Morocco. *Geological Society, London, Special Publications*, *132*(1), 283-296. DOI: 10.1144/GSL.SP.1998.132.01.16

Müller, R. D., Sdrolias, M., Gaina, C., Roest, W. R., 2008. Age, spreading rates, and spreading asymmetry of the world's ocean crust. Geochemistry, Geophysics, Geosystems, 9(4). DOI: 10.1029/2007GC001743

Neumaier, M., Back, S., Littke, R., Kukla, P. A., Schnabel, M., Reichert, C., 2016. Late Cretaceous to Cenozoic geodynamic evolution of the Atlantic margin offshore Essaouira (Morocco). *Basin Research*, *28*(5), 712-730. DOI: 10.1111/bre.12127

Nye, J. F., 1952. The mechanics of glacier flow. *Journal of Glaciology*, *2*(12), 82-93.

Peron-Pinvidic, G., Manatschal, G., Osmundsen, P. T., 2013. Structural comparison of archetypal Atlantic rifted margins: A review of observations and concepts. *Marine and petroleum geology*, *43*, 21-47. DOI: 10.1016/j.marpetgeo.2013.02.002

Péron-Pinvidic, G., Manatschal, G., Masini, E., Sutra, E., Flament, J. M., Haupert, I., Unternehr, P., 2017. Unravelling the along-strike variability of the Angola–Gabon rifted margin: a mapping approach. *Geological Society, London, Special Publications*, *438*(1), 49-76. DOI: 10.1144/SP438.1

Pichel, L. M., Huuse, M., Redfern, J., Finch, E., 2019. The influence of base-salt relief, rift topography and regional events on salt tectonics offshore Morocco. *Marine and Petroleum Geology*, *103*, 87-113. DOI: 10.1016/j.marpetgeo.2019.02.007

Piqué, A., Le Roy, P., Amrhar, M., 1998. Transtensive synsedimentary tectonics associated with ocean opening: the Essaouira–Agadir segment of the Moroccan Atlantic margin. *Journal of the Geological Society*, *155*(6), 913-928. DOI: 10.1144/gsjgs.155.6.0913

Quirk, D. G., Schødt, N., Lassen, B., Ings, S. J., Hsu, D., Hirsch, K. K., Von Nicolai, C., 2012. Salt tectonics on passive margins: examples from Santos, Campos and Kwanza basins. *Geological Society, London, Special Publications*, *363*(1), 207-244.

Ramberg, H., 1981. The role of gravity in orogenic belts. *Geological Society, London, Special Publications*, *9*(1), 125-140.

Ranke, U., von Rad, U., Wissmann, G., 1982. Stratigraphy, facies and tectonic development of the on- and offshore Aaiun-Tarfaya Basin - A review. In: von Rad U., Hinz K., Sarnthein M., Seibold E. (eds) Geology of the Northwest African Continental Margin. Springer, Berlin, Heidelberg.

Ratschiller, L. K.,1968. Lithostratigraphy of the northern Spanish Sahara. Trento: Museo Tridentino di Scienze Naturali.

Robertson, A. H. F., Stillman, C. J., 1979. Late Mesozoic sedimentary rocks of Fuerteventura, Canary Islands: implications for West African continental margin evolution. Journal of the Geological Society, 136(1), 47-60. DOI: 10.1144/gsjgs.136.1.0047

Roeser, H. A., Steiner, C., Schreckenberger, B., Block, M., 2002. Structural development of the Jurassic Magnetic Quiet Zone off Morocco and identification of Middle Jurassic magnetic lineations. *Journal of Geophysical Research: Solid Earth*, *107*(B10), EPM-1. DOI: 10.1029/2000JB000094

Roeser, H. A., 1982. Magnetic anomalies in the magnetic quiet zone off Morocco. In: von Rad U., Hinz K., Sarnthein M., Seibold E. (eds) Geology of the Northwest African Continental Margin. Springer, Berlin, Heidelberg. DOI: 10.1007/978-3-642-68409-8_4

Roma, M., Ferrer, O., McClay, K. R., Muñoz, J. A., Roca, E., Gratacós, O., and Cabelllo, P., 2018. Weld kinematics of syn-rift salt during basement-involved extension and subsequent inversion: Results from analog models. *Geologica Acta: an international earth science journal,* 16(4), 391-410. DOI: 10.1344/GeologicaActa2018.16.4.4

Rowan, M. G., 1993. A systematic technique for the sequential restoration of salt structures. Tectonophysics, 228(3-4), 331-348.

Rowan, M. G., Peel, F., Vendeville, B., 2004. Gravity-driven Fold Belts on Passive Margins, In: K. R. McClay (ed.) Thrust Tectonics and Hydrocarbon Systems (pp. 157-182). AAPG Memoir 82. DOI: 10.1306/M82813C9

Rowan, M. G., Inman, K. F., 2005. Counterregional-style deformation in the deep shelf of the northern Gulf of Mexico. Gulf Coast Association of Geological Societies Transactions, 55, 716-724.

Rowan, M. G., Peel, F. J., Vendeville, B. C., Gaullier, V., 2012. Salt tectonics at passive margins: Geology versus models–Discussion. Marine and Petroleum Geology, 37(1), 184-194.

Rowan, M. G., 2014. Passive-margin salt basins: Hyperextension, evaporite deposition, and salt tectonics. Basin Research, 26(1), 154-182. DOI: 10.1111/bre.12043

Rowan, M. G. Krzywiec, P., 2014. The Szamotuły salt diapir and Mid-Polish Trough: decoupling during both Triassic-Jurassic rifting and Alpine inversion. *Interpretation*, *2*(4), SM1-SM18.

Rowan, M. G., 2017. An overview of allochthonous salt tectonics.In: Soto J., Flinch J., & Tari G. (eds.) Permo-Triassic Salt Provinces of Europe, North Africa and the Atlantic Margins. Tectonics and Hydrocarbon Potential (pp. 97-114). Elsevier. DOI: 10.1016/B978-0-12-809417-4.00005-7

Rowan, M. G., Lindsø, S., 2017. Salt tectonics of the Norwegian Barents Sea and northeast Greenland shelf. In: Soto J., Flinch J., & Tari G. (eds.) *Permo-Triassic Salt Provinces of Europe, North Africa and the Atlantic Margins* (pp. 265-286). Elsevier. DOI: 10.1016/B978-0-12-809417-4.00013-6

Rowan, M. G., 2018. The South Atlantic and Gulf of Mexico salt basins: crustal thinning, subsidence and accommodation for salt and presalt strata. In: McClay, K. R. & Hammerstein, J. A. (eds) Passive Margins: Tectonics, Sedimentation and Magmatism. Geological Society, London, Special Publications, 476(1), 333-363. DOI: 10.1144/SP476.6

Rowan, M. G., Jarvie, A., 2020. Crustal extension and salt tectonics of the Danmarkshavn Ridge and adjacent basins, NE Greenland. Marine and Petroleum Geology, 117, 104339. DOI: 10.1016/j.marpetgeo.2020.104339

Rowan, M. G., 2020a. The South Atlantic and Gulf of Mexico salt basins: crustal thinning, subsidence and accommodation for salt and presalt strata. *Geological Society, London, Special Publications*, *476*(1), 333-363. DOI: 10.1144/SP476.6

Rowan, M. G., 2020b. Salt-and shale-detached gravity-driven failure of continental margins. In: Scarselli, N., Adam, J., & Chiarella, D. (eds.) *Regional Geology and Tectonics* (pp. 205-234). Elsevier. DOI: 10.1016/B978-0-444-64134-2.00010-9

Rowan, M. G., 2021. The ocean-continent transition of late synrift salt basins: extension and evaporite deposition in the southern Gulf of Mexico and global analogs. Accepted for publication in GSA Special Paper, to honor W. Alvarez, 'From the Guajira Desert to the Apennines, and from Mediterranean microplates to the Mexican killer asteroid'.

Ruiz, G. M. H., Sebti, S., Negro, F., Saddiqi, O., Frizon de Lamotte, D., Stockli, D., Foeken, F., Stuart, F, Barbarand, J., Schaer, J. P., 2011. From central Atlantic continental rift to Neogene uplift–western Anti-Atlas (Morocco). *Terra Nova*, *23*(1), 35-41. DOI: 10.1111/j.1365-3121.2010.00980.x

Sachse, V. F., Wenke, A., Littke, R., Jabour, H., Kluth, O., Zühlke, R., 2016. 2D petroleum system analysis of the Tarfaya Basin, on-offshore Morocco, North Africa. *Marine and Petroleum Geology*, *77*, 1108-1124. DOI: 10.1016/j.marpetgeo.2020.104339

Sahabi, M., Aslanian, D., Olivet, J. L., 2004. Un nouveau point de départ pour l'histoire de l'Atlantique central. *Comptes Rendus Geoscience*, *336*(12), 1041-1052. DOI: 10.1016/j.crte.2004.03.017

Sapin, F., Ringenbach, J. C., Clerc, C., 2021. Rifted margins classification and forcing parameters. *Scientific Reports*, *11*(1), 1-17.

Schettino, A., Turco, E., 2009. Breakup of Pangaea and plate kinematics of the central Atlantic and Atlas regions. *Geophysical Journal International*, *178*(2), 1078-1097.

Schettino, A., Turco, E., 2011. Tectonic history of the western Tethys since the Late Triassic. *Bulletin*, *123*(1-2), 89-105. DOI: 10.1130/B30064.1

Schultz-Ela, D. D., 2001. Excursus on gravity gliding and gravity spreading. *Journal of structural geology*, *23*(5), 725-731. DOI: 10.1016/S0191-8141(01)00004-9

Sehrt, M., 2014. *Variscan to Neogene long-term landscape evolution at the Moroccan passive continental margin (Tarfaya Basin and western Anti-Atlas)* (Doctoral dissertation, Heidelberg). DOI: 10.11588/heidok.00017463

Sehrt, M., Glasmacher, U. A., Stockli, D. F., Jabour, H., Kluth, O., 2018. The southern Moroccan passive continental margin: An example of differentiated long-term landscape evolution in Gondwana. *Gondwana Research*, *53*, 129-144. DOI: 10.1016/j.gr.2017.03.013

Seibold, E., 1982. The northwest African continental margin—An introduction. In: von Rad U., Hinz K., Sarnthein M., Seibold E. (eds) *Geology of the Northwest African Continental Margin* (pp. 3-20). Springer, Berlin, Heidelberg. DOI: 10.1007/978-3-642-68409-8_1

Sibuet, J. C., Rouzo, S., Srivastava, S., 2012. Plate tectonic reconstructions and paleogeographic maps of the central and North Atlantic oceans. *Canadian Journal of Earth Sciences*, *49*(12), 1395-1415. DOI: 10.1139/e2012-071

Steiner, C., Hobson, A., Favre, P., Stampfli, G. M., Hernandez, J., 1998. Mesozoic sequence of Fuerteventura (Canary Islands): Witness of Early Jurassic sea-floor spreading in the central Atlantic. *Geological Society of America Bulletin*, *110*(10), 1304-1317. DOI: 10.1130/0016-7606(1998)110<1304:MSOFCI>2.3.CO;2

Stets, J., Wurster, P., 1982. Atlas and Atlantic—structural relations. In: von Rad U., Hinz K., Sarnthein M., Seibold E. (eds) *Geology of the Northwest African continental margin* (pp. 69-85). Springer, Berlin, Heidelberg. DOI: 10.1007/978-3-642-68409-8_5

Stica, J. M., Zalán, P. V., Ferrari, A. L., 2014. The evolution of rifting on the volcanic margin of the Pelotas Basin and the contextualization of the Paraná–Etendeka LIP in the separation of Gondwana in the South Atlantic. *Marine and Petroleum Geology*, *50*, 1-21.

Tari, G., Molnar, J., Ashton, P., Hedley, R., 2000. Salt tectonics in the Atlantic margin of Morocco. *The Leading Edge*, *19*(10), 1074-1078. DOI: 10.1144/SP369.23

Tari, G., Molnar, J., Ashton, P., 2003. Examples of salt tectonics from West Africa: a comparative approach. *Geological Society, London, Special Publications*, *207*(1), 85-104. DOI: 10.1144/GSL.SP.2003.207.5

Tari, G., Brown, D., Jabour, H., Hafid, M., Louden, K., Zizi, M., 2012a. The conjugate margins of Morocco and Nova Scotia. In: D.G. Roberts & A.W. Bally (eds.) Regional Geology and Tectonics: Phanerozoic Passive Margins, Cratonic Basins and Global Tectonic Maps (pp. 285–323). Elsevier, Amsterdam.

Tari, G., Jabour, H., Molnar, J., Valasek, D., Zizi, M., 2012b. Deep-water exploration in Atlantic Morocco: Where are the reservoirs? In: Gao, D. (ed.) Tectonics and sedimentation: Implications for petroleum systems (pp. 337-355). AAPG Memoir 100. DOI:10.1306/13351560M1003141

Tari, G., Jabour, H., 2013. Salt tectonics along the Atlantic margin of Morocco. *Geological Society, London, Special Publications*, *369*(1), 337-353. DOI: 10.1144/SP369.23

Tari, G., Novotny, B., Jabour, H., Hafid, M., 2017. Salt tectonics along the Atlantic margin of NW Africa (Morocco and Mauritania). In Soto, J. I., Flinch, J., & Tari, G. (eds.) Permo-Triassic salt provinces of Europe, North Africa and the Atlantic margins (pp. 331-351).

Tugend, J., Manatschal, G., Kusznir, N. J., Masini, E., 2015. Characterizing and identifying structural domains at rifted continental margins: application to the Bay of Biscay margins and its Western Pyrenean fossil remnants. *Geological Society, London, Special Publications*, *413*(1), 171-203. DOI: 10.1144/SP413.3

Tugend, J., Gillard, M., Manatschal, G., Nirrengarten, M., Harkin, C., Epin, M. E., Sauter, D., Autin, J., Kusznir, N., Mcdermott, K., 2020. Reappraisal of the magma-rich versus magma-poor rifted margin archetypes. *Geological Society, London, Special Publications*, *476*(1), 23-47. DOI: 10.1144/SP476.9

Uchupi, E., Emery, K. O., Bowin, C. O., Phillips, J. D., 1976. Continental margin off western Africa: Senegal to Portugal. *AAPG Bulletin*, *60*(5), 809-878. DOI: 10.1306/C1EA35BE-16C9-11D7-8645000102C1865D

van den Bogaard, P. (2013). The origin of the Canary Island Seamount Province-New ages of old seamounts. Scientific Reports, 3(1), 1-7.

Vendeville, B. C., Nilsen, K. T., 1995. Episodic growth of salt diapirs driven by horizontal shortening. Salt, sediment and hydrocarbons: Gulf Coast Section SEPM Foundation 16th Annual Research Conference. 285-295.

Vendeville, B. C., 2005. Salt tectonics driven by sediment progradation: Part I—Mechanics and kinematics. *AAPG bulletin*, *89*(8), 1071-1079. DOI: 10.1306/03310503063

Wagner III, B. H., Jackson, M. P., 2011. Viscous flow during salt welding. *Tectonophysics*, *510*(3-4), 309-326. DOI: 10.1016/j.tecto.2011.07.012

Wenke, A., 2014. Sequence stratigraphy and basin analysis of the Tarfaya-Laâyoune Basins Morocco, on-and offshore Morocco (Doctoral dissertation, Heidelberg). DOI: 10.11588/heidok.00017905

Zühlke, R., Bouaouda, M. S., Ouajhain, B., Bechstädt, T., Leinfelder, R., 2004. Quantitative Meso-/Cenozoic development of the eastern central Atlantic continental shelf, western High Atlas, Morocco. *Marine and Petroleum Geology*, *21*(2), 225-276. DOI: 10.1016/j.marpetgeo.2003.11.014